
Techniques to reduce the Mutual Coupling and to improve the Isolation between antennas in a Diversity System

Department of Electronic Systems
Antennas Propagation and Radio Networking
10th semester
Aalborg University 2009
Group 09gr995

Abstract:

Title:

Techniques to reduce the Mutual Coupling and to improve the Isolation between antennas in a Diversity System

Project period:

E10, Autumn semester 2009

Project group:

09gr995

Participants:

Javier Pablos Abelairas
Fabián Molina Martín

Supervisor:

Mauro Pelosi
Gert Frølund Pedersen

Copies: 3

Date of completion: January 6th, 2010

In recent years demanding of new applications and services for mobile devices has seen a great increment. These new applications need a bigger bit rate to work properly. In this scenario several MIMO (Multiple In-Multiple Out) systems are being implemented. In MIMO systems, multiple antennas are located inside the devices to take advantage of the diversity that these systems provide. A condition to achieve this purpose is based on the relation between antennas, this means low correlation and high isolation. The problem with mobile devices due to their small size is the short distance between antennas that increase correlation and reduces isolation.

This thesis is focussed on the investigation of an optimal solution that improves isolation of antennas in mobile phone handsets.

To this purpose three types of antennas have been used : ILA, Inverted-L Antenna, IFA, Inverted-F Antenna, and PIFA, Planar Inverted-F Antenna. And two methods to increase the isolation has been tested: Dielectric walls and dielectric ground plane DGP.

Javier Pablos Abelairas

<jabuti@es.aau.dk>

Fabián Molina Martín

<fabian@es.aau.dk>

Preface

This following master thesis is written by project group 09gr995 at the Section of Telecommunications, Department of Electronic Systems at Aalborg University during the 10th semester of the master programme in the period spanning from September 1st, 2009 to January 5th, 2010. The thesis concerns the investigation of an optimal solution that improves isolation of antennas in mobile phone handsets.

The report is aimed at people with knowledge equivalent to the teaching on the 4th semester master programme in mobile communications. The project “Techniques to reduce the Mutual Coupling and to improve the Isolation between antennas in a Diversity System” has been proposed by Mauro Pelosi.

We would like to thank our project supervisors, Gert Frølund Pedersen and Mauro Pelosi, for their guidance and time throughout this project.

The reader should pay attention to the following when examining this report:

- The report is divided into two major parts:
 - The main report which is divided into numbered chapters.
 - The appendices which are arranged alphabetically.
- Figures, tables and equations are enumerated consecutively according to the chapter’s number. Hence, the first figure in chapter one is named Figure 1.1, the second figure Figure 1.2 and so on.

Aalborg University, June 3rd 2009.

Table of Contents

1	Introduction	2
2	Project Description	4
2.1	Project Scope	4
2.2	Report Structure	4
2.3	Simulation environment	5
3	Study of single antenna systems	6
3.1	All band antennas	6
3.2	Reception and transmission antennas	22
3.3	UMTS band <i>I</i> , band <i>II</i> and band <i>V</i> antennas	23
4	Study of dual antenna systems	26
4.1	Study based on the antenna features	27
4.2	Uplink and Downlink antennas	29
4.3	Antennas for Clamshell handsets	30
5	Techniques to improve isolation	32
5.1	Dielectric Walls	33
5.2	Defected Ground Plane DGP	40
6	Conclusions	52
	Bibliography	53
	Appendix	55
A	Evolution of mobile cellular network	58
A.1	First-Generation Mobile Systems 1G	58
A.2	Second-Generation Mobile Systems 2G	58
A.3	Second and a half-Generation Mobile Systems 2.5G	59
A.4	Third-Generation Mobile Systems 3G	59
A.5	Universal Mobile Telecommunications System UMTS	59

B Monopole Theory	60
B.1 Inverted-L Antenna ILA	61
B.2 Inverted-F Antenna IFA	61
B.3 Planar Inverted-F Antenna PIFA	62
C Finite-Differences Time-Domain FDTD	64
C.1 3rd generation FDTD program	66
D MIMO Systems	70
D.1 Fundamentals of MIMO	70
D.2 Benefits of MIMO technology	71

Introduction

In recent years demanding of new applications and services for mobile devices has seen a great increase. These new applications need a bigger bit rate to work properly, however not only the bit rate is important, design and services that one device can provide to the user are also important. Nowadays, it is normal to see mobile phones with the possibility of multiple services as GPS, WIFI, Bluetooth, Infrared. All this services need an antenna to transmit and receive data.

For optimum system performance, the antennas must have high radiation efficiency, small volume, isotropic radiation characteristics, simple and low-loss impedance matching to the receive and transmit paths, and simple mechanical construction. Therefore it is necessary to design properly the antennas of the handset and to take into account important parameters, because changing the physical dimensions of the antenna will also affect on its efficiency and bandwidth [18].

In the current industry, the antenna requirements for a handset has evolved from a single main antenna to multiantenna solutions, as Multiple-Input Multiple-Output systems (MIMO). In MIMO systems, multiple antennas are located inside the devices to take advantage of the diversity that these systems provide. Array gain, spatial diversity gain, spatial multiplexing gain and interference reduction are some of its advantages.

The main problem in MIMO systems for mobile handsets is the short distance between the antennas because when two or more antennas are located in close proximity, mutual coupling can occur between them. This can result in degradation of their radiation patterns and changes in the input impedance. Several techniques to reduce the mutual coupling and improve the isolation are being investigated.

Another issue to take into consideration is that when mobile phones are used in close proximity with the human body, this results in a detrimental effect in its communication performances [3].

Chapter 2

Project Description

2.1 Project Scope

This master thesis concerns the investigation of an optimal solution that reduces the mutual coupling and improves the isolation between antennas in mobile phone handsets.

For this purpose, three types of antennas have been used : Inverted-L Antenna ILA, Inverted-F Antenna IFA, and Planar Inverted-F Antenna PIFA. And two methods to increase the isolation has been tested: Dielectric walls and Defected Ground Planes DGP.

2.2 Report Structure

This report try to be a essential manual to understand the behaviour of the different antennas and the isolation techniques. For future users this report can be a quick guide to start to investigate on MIMO systems and ILA, IFA and PIFA antennas.

The structure of this report is as follows:

- Simulations: In this part technical work of the project is going to be explained. User will find here a briefing of the simulations results that will help to understand the behaviour of the antennas in mobile phone systems. It is divided in three parts:
 - Study of single antenna systems (chapter 3): Describes the structure of a simple antenna and discusses the relationship between its various parameters.
 - Study of dual antenna systems (chapter 4): Systems with two antennas in the same printed circuit board are introduced.
 - Techniques to improve isolation (chapter 5): Some techniques to improve the isolation between antennas are expounded.
- Conclusions (chapter 6): In this chapter is summarized the work done on this project and the results obtained are discussed. Possible future works are also commented.

- Appendix: All the background needed to understand the work done in this project can be founded here.

2.3 Simulation environment

To make the required simulations to investigate the mutual antenna decoupling system, it was used a Finite-Difference Time-Domain (see Appendix C) code deployed at Aalborg University called AAU3.

The supercomputer Fyrkat executed the simulations. Thanks to Fyrkat, a lot of time in executing the simulations was saved. One simulation launched on Fyrkat has a duration of around 2-3 hours. The same simulation without Fyrkat take more time (e.g. various days) and is less accurate. More information about Fyrkat can be found in [1].

For the simulations the scenario consists of one or two antennas placed on top of a small ground plane whose size is the same as the normal size of the Printed Circuit Board (PCB) of a typical mobile handset. The dimensions of the PCB are $100mm \times 40mm$ for a “candy bar” phone and $200mm \times 40mm$ for a “clamshell” phone.

It is assumed that our scenario is an isotropic network, therefore S_{21} is equal to S_{12} . Moreover in further results we only show S_{21} as they are the same.

Chapter 3

Study of single antenna systems

This chapter will introduce the selected antennas for the simulations. They are the Inverted-L Antennas (ILA), the Inverted-F Antennas (IFA) and the Planar Inverted-F Antennas (PIFA)(see Apendix B). There are three different sections. The first one shows how the behaviour of the antenna varies, specifically the S_{11} parameter, when some of its physical characteristics (length, height, position of the feed, etc.) are modified. Using that knowledge it is also shown how to achieve a good input impedance matching of the antenna. Antennas used in this section cover all the bandwidth of UMTS band *I*. Besides, the problem in this systems is that if a signal transmitted by a handset reaches a simultaneously operating receiver in the same handset at a strong enough level, it can saturate that receiver, and prevent it from receiving information. Therefore, the second section shows antennas designed to cover only the uplink or the downlink of the UMTS band *I*. Finally, the third section compares the dimensions of antennas designed for UMTS band *I*, band *II* and band *V*.

3.1 All band antennas

3.1.1 ILA and IFA antennas

Both ILA and IFA are monopoles that have been folded at a certain point. From that point the antenna is parallel to the ground plane. Its total length is the sum of the two sides of the antenna, the vertical, perpendicular to the ground plane, and the horizontal, parallel to it. For a monopole this total length is often $\lambda/4$. It is possible to select the resonance frequency by adjusting this length L , in which the antenna works.

$$\left. \begin{array}{l} L = \frac{\lambda}{4} \\ \lambda = \frac{c}{f} \end{array} \right\} \implies f = \frac{c}{4L} \quad (3.1)$$

where

- L : Total length of the antenna [m].
- λ : Wavelength [m].
- f : Frequency [Hz].
- c : Vacuum light speed $3 \cdot 10^8$ [m/s].

The following section shows how to modify the length and width to obtain a good match.

Modifying ILA features

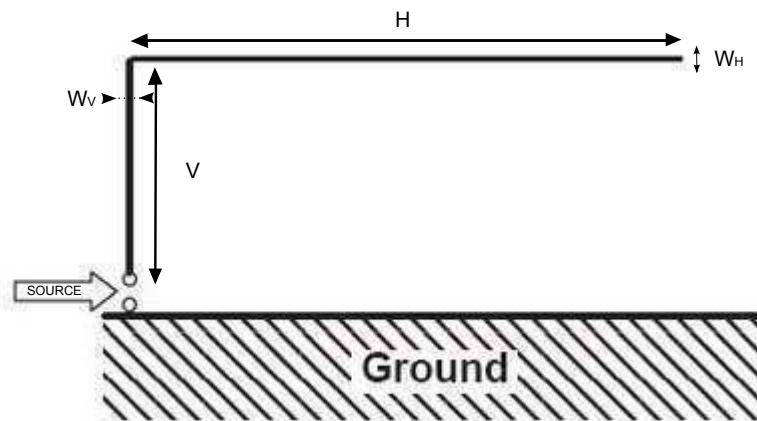


Figure 3.1: ILA scheme [25].

The ILA parameters that are going to be modified to evaluate its behaviour are:

- Vertical length V and width W_V .
- Horizontal length H and width W_H .

From equation 3.1, as the antenna has to resonate at 2100 MHz, it is obtained that the theoretical total length should be 35.71mm.. Then, the horizontal length H is modified, keeping the same vertical length V . The inverted process is also done, this means that H is maintained and V is modified. The results can be seen in Figure 3.2. As it is expected, making longer the horizontal or vertical lengths, the resonance frequency shifts to lower values (see equation 3.1), but better results are obtained making longer the vertical length than extending the horizontal one, because the value of the S_{11} parameter is lower at the resonance frequency and the bandwidth at -6 dB is greater.

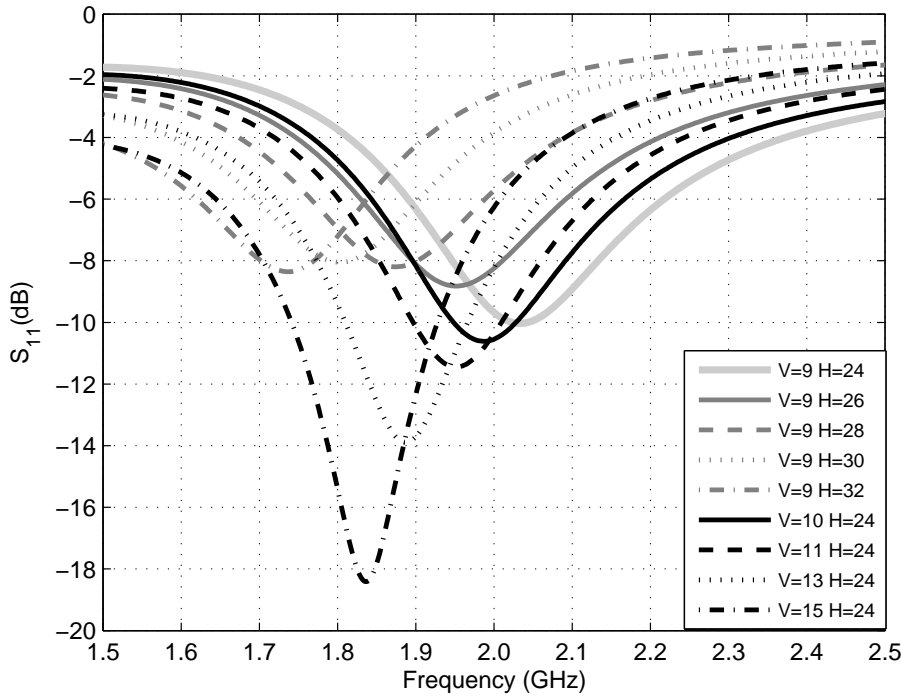


Figure 3.2: S_{11} in an ILA antenna when H and L lengths are modified separately.

Then both vertical and horizontal lengths are modified at the same time in order to keep the total length. Therefore the resonance frequency is the same for all antennas. Once again, as it is depicted in Figure 3.3 the longer the vertical arm of the antenna, the deeper the S_{11} function at the resonance frequency is. Similarly, the bandwidth increases.

Other parameter that can be modified is the width of the arms. Widths of 1mm. , 2mm. and 3mm. are used in each arm of the ILA. Figure 3.4 shows S_{11} of an ILA ($V = 9\text{mm.}$ and $H = 24\text{mm.}$) versus an ILA with modified arms.

Modifying IFA features

IFA antenna is a modification of an ILA antenna. A small ILA element has been attached at the end of its vertical element. Therefore the parameters to modify in these antennas, presented in Figure 3.5, are:

- Vertical length V and width W_V .
- Horizontal length H and width W_H .
- Distance S between the source ILA and the vertical arm of the attached ILA.

Figure 3.6 illustrates the different behaviour between ILA and IFA antennas, due to the addition of the short. Both antennas have the same size. It is also shown how the input impedance matching varies when the distance between the short and the source S is modified.

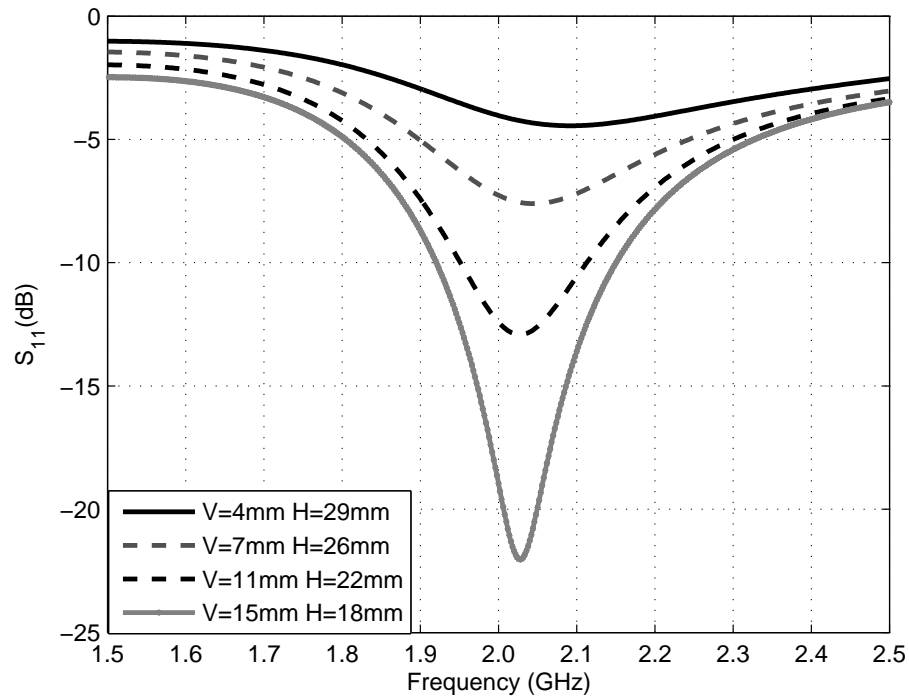


Figure 3.3: S_{11} in an ILA antenna when H and V lengths are modified at the same time to keep the same total length.

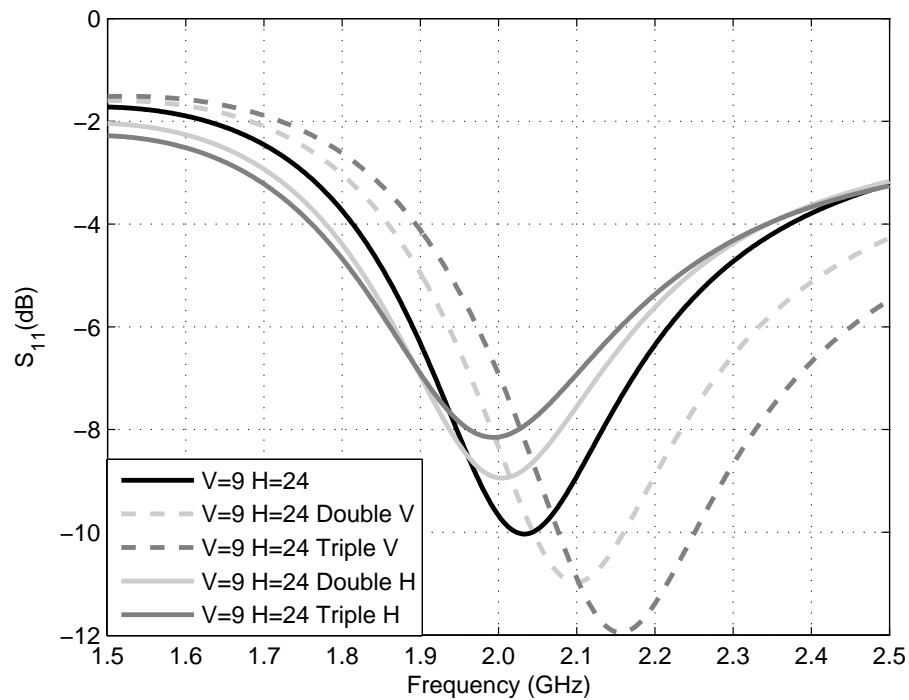


Figure 3.4: S_{11} in an ILA antenna when H and V widths are modified. The widths are $W_H = 2, 3\text{mm}$. and $W_V = 2, 3\text{mm}$.

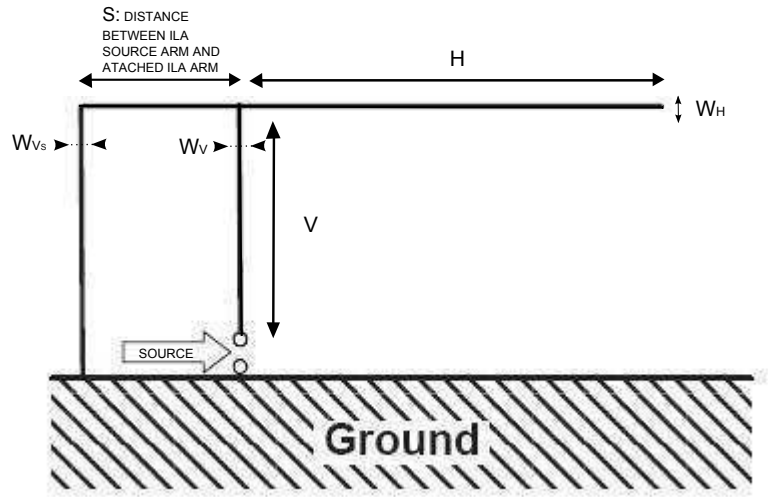


Figure 3.5: IFA scheme [25].

As it was done for ILA antennas, the first step is to change just the horizontal length H , keeping the same vertical length V . Furthermore, the reverse process is done, i.e. the horizontal length is fixed and the vertical one is modified. The results are shown in Figure 3.7.

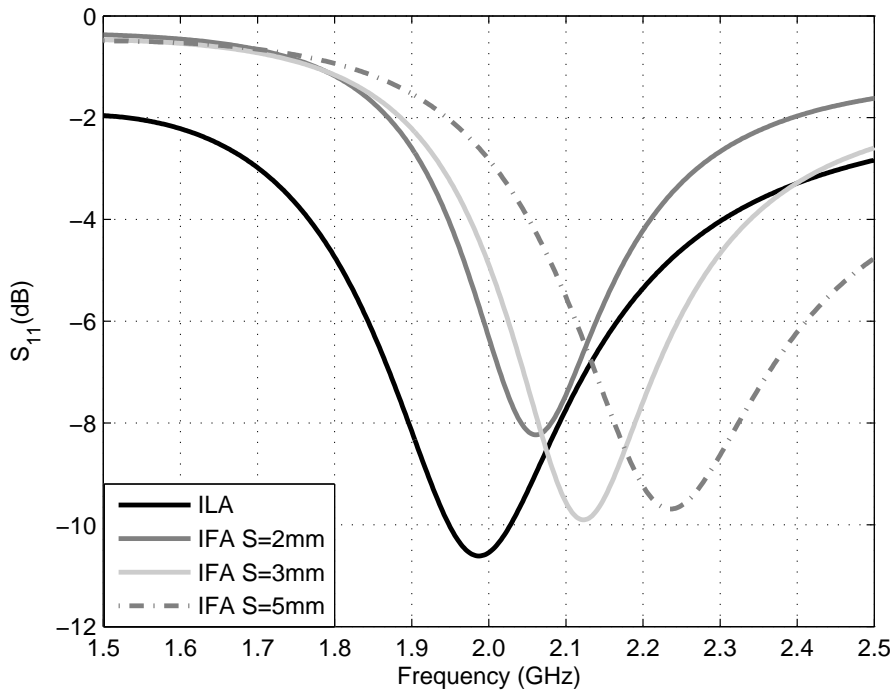


Figure 3.6: ILA versus IFA. S is the distance between the short and the source pin of the IFA.

Since IFA is a monopole, the resonance frequency increases its value when the horizontal or vertical lengths are increased (equation 3.1), but in contrast to ILA antennas (Figure 3.2), better results are obtained by raising H instead of V . Again, the value of the S_{11} parameter is lower at the resonance frequency and the bandwidth at -6 dB is greater.

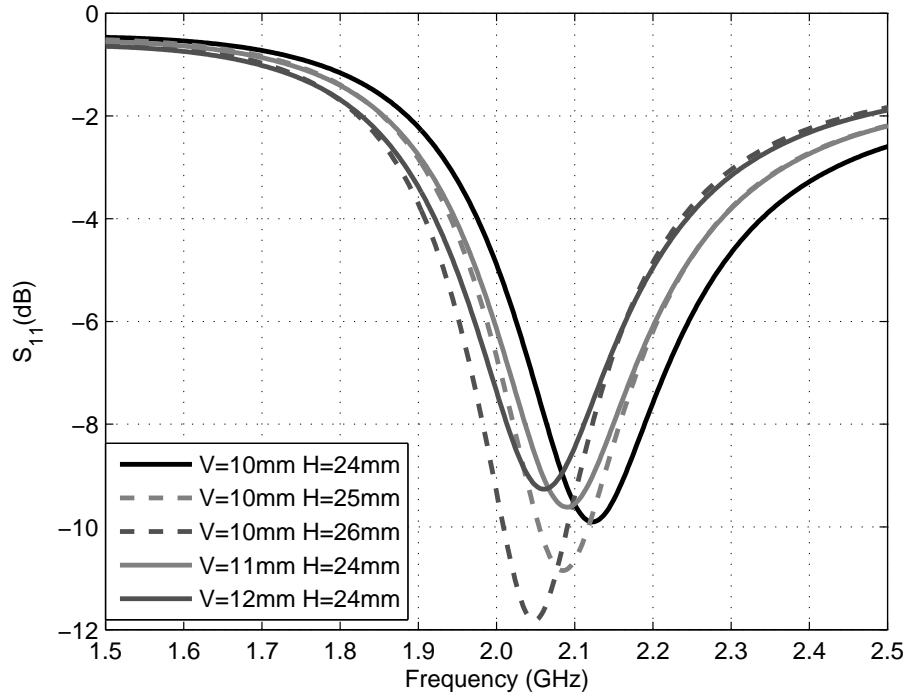


Figure 3.7: S_{11} in an IFA antenna when H and V lengths are modified separately. In all cases $S=3\text{mm}$.

Then both vertical and horizontal lengths are changed, keeping in this case the total length and thus the resonance frequency is the same.

The next step is to increase the width of the arms of the antenna, starting with the horizontal arm. This horizontal arm can be divided in two parts:

1. The part between the short and the source pin S
2. The part of the original ILA antenna H

Based on mentioned above, in Figure 3.8 these three different simulations are displayed:

1. Change only the width of H .
2. Change only the width of S .
3. Change both parameters.

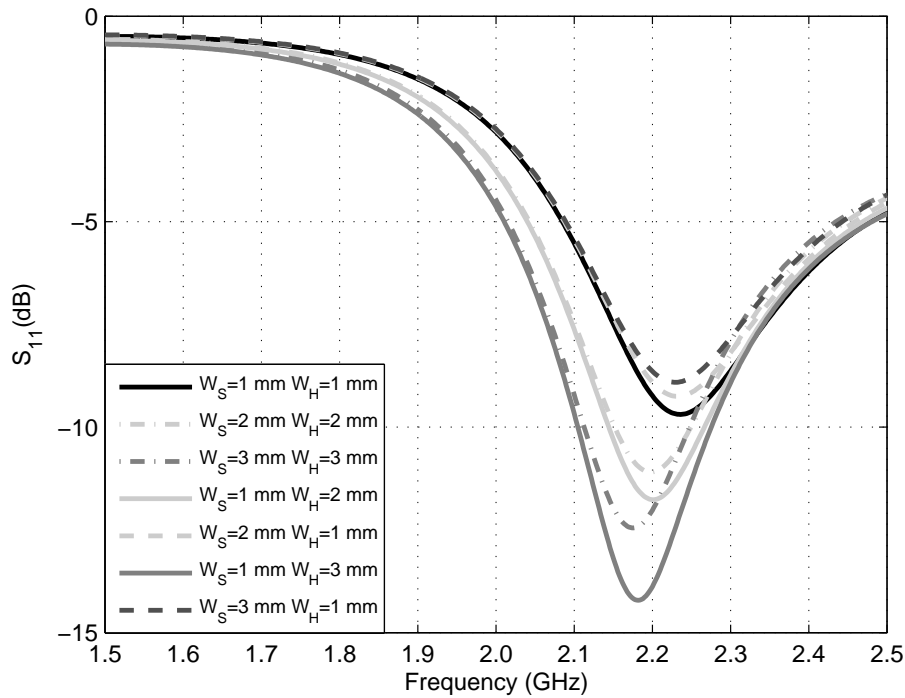


Figure 3.8: Changes in S_{11} when H and S widths are modified at the same time.

In this case the best option to enhance the bandwidth and improve the matching, is to make wider only the horizontal arm. Increasing the length of the horizontal arm and the distance between the short and the source has the same effects as mentioned before but the improvements are not so good as before. If S is the only changed parameter, then there is no effect on the matching neither the bandwidth.

The following test gives an idea of how the parameter S_{11} changes when the width of the vertical arms are modified. As IFA antenna has two vertical arms, henceforth they will be called V and V_{short} . Their widths are increased separately.

Figure 3.9 shows that is better to modify only the width of the vertical arm of the source. Increasing this width a better input impedance matching and a greater bandwidth is obtained. On the contrary modifying the width of the short, the results are worse, the matching and the bandwidth are decreased without any other benefit.

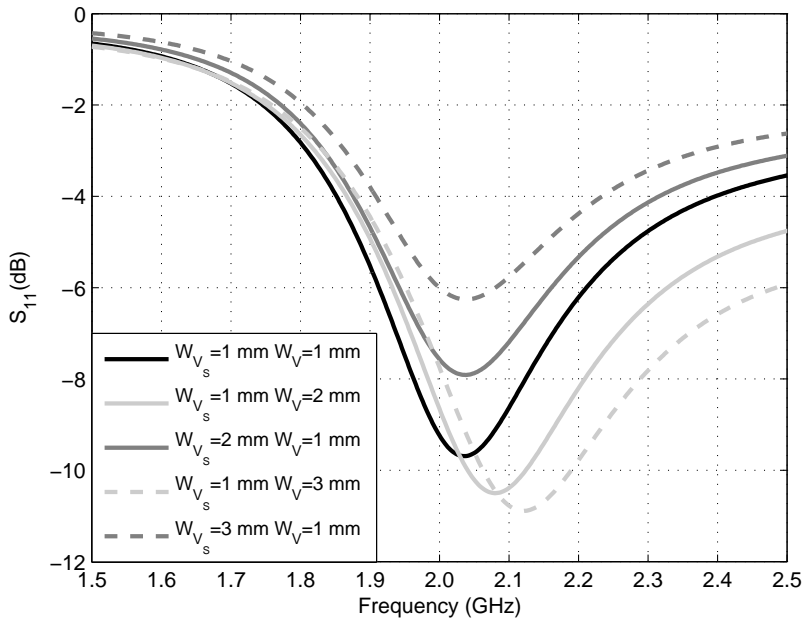


Figure 3.9: S_{11} in an IFA antenna when the widths of V and V_s are modified.

Common Features

In this section some tests of the features that are common to ILA and IFA antennas are presented. These features are the position of the antenna on the ground plane and the dimensions of the ground plane.

Ground plane dimensions: Only two standard dimensions for the ground plane are used in this project, the first and most used is a rectangle which length is 100mm . and its width 40mm . In this case the ground plane is simulated as a typical 'candy bar' phone. The second one has the typical dimensions of a 'clamshell' phone, i.e. 200mm length and 40mm width. Both mobile phones are presented in Figure 3.10.

Although only candy bar and clamshell phones dimensions are used, the following test shows the different results when the ground plane is modified. A typical ILA antenna configuration is used. Figure 3.11 depicts a scheme of the ground planes used for the test and Figure 3.12 shows the results.

In this case if only the S_{11} value is taken into account, the ground plane with dimensions 100mm x 45mm has a better input impedance matching, but as mentioned before only two specific dimensions of the ground plane are used to make the simulations closer to real mobile phones.

Position over the ground plane: The following test examines what should be the position of the antenna within the ground plane. Recent studies have determined that the best position to put the antennas in the ground plane is at the corners, due to the electric field of ground plane resonant modes would be maximal in these locations [28]. In this case the sources of the antenna are placed at the corners of the ground plane but changing the orientation of the arms, as illustrated in Figure 3.13. Moreover, Figure 3.14 provides the results of the test.



Figure 3.10: Different shapes of the simulated mobile phones: a) Candy bar phone b) Clamshell phone

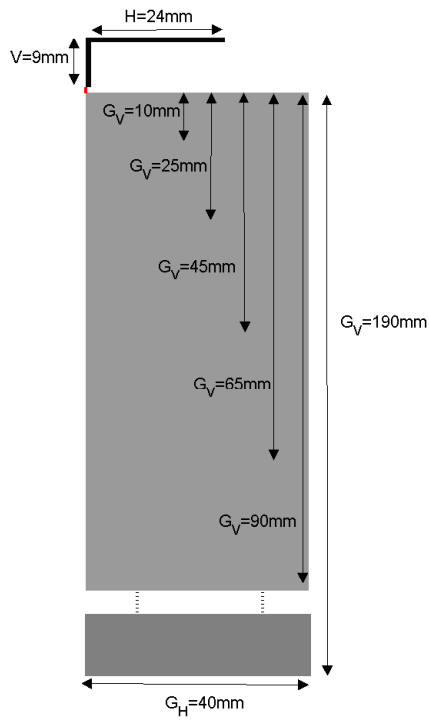


Figure 3.11: Lengths of the ground plane that are used in the test

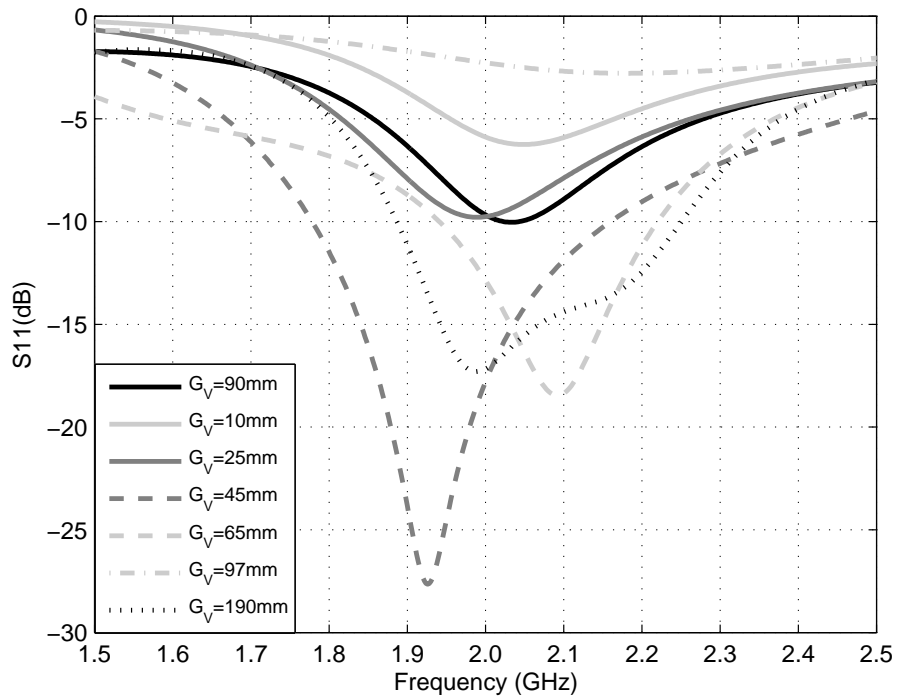


Figure 3.12: S_{11} of an ILA antenna when the ground plane dimensions are modified.

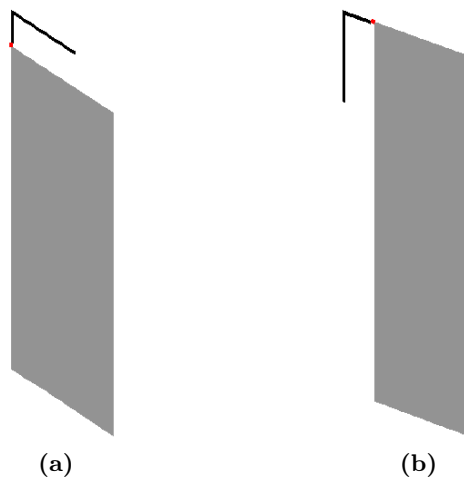


Figure 3.13: Different antenna placements tested

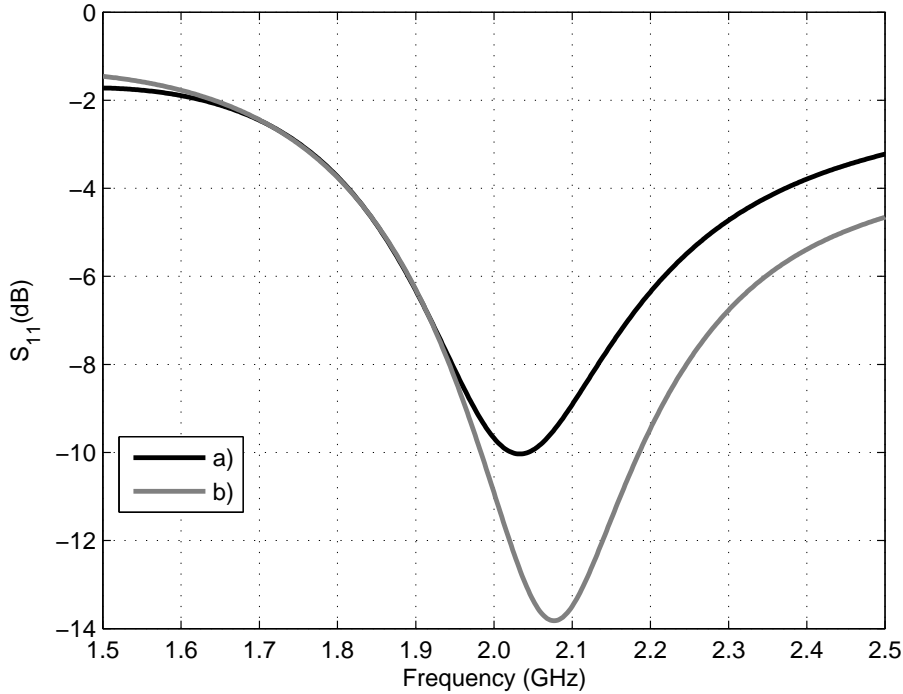


Figure 3.14: S_{11} of an ILA antenna depending on the position of the antenna in the ground plane.

As it can be seen in Figure 3.14, the position (b) has the best input impedance matching maybe not for placement but for the size of the ground plane, as it was shown in the previous paragraph. Anyway, placement (a) is chosen for the simulation due to its similarity to real mobile phones.

3.1.2 PIFA antenna

PIFA can be considered as a kind of linear Inverted F antenna (IFA) with the wire radiator element replaced by a plate to expand the bandwidth. It is essentially a $\lambda/4$ resonant inverted F microstrip patch shorted at one end.

The resonance frequency of a PIFA antenna depends on some parameters shown in Figure 3.15. It is possible to compute it using the equation 3.2 which states that the dimension of the top plate are inversely proportional to the resonant frequency.

$$F_r = \frac{c}{4 \cdot (L_1 + L_2 + h - W)} \quad (3.2)$$

where

- F_r : Resonance frequency [Hz].
- L_1 : Length of the PIFA antenna [m].
- L_2 : Width of the PIFA antenna [m].

- h : Height of the PIFA antenna [m].
- W : Width of the shorting plate [m].
- c : Vacuum light speed $3 \cdot 10^8$ [m/s].

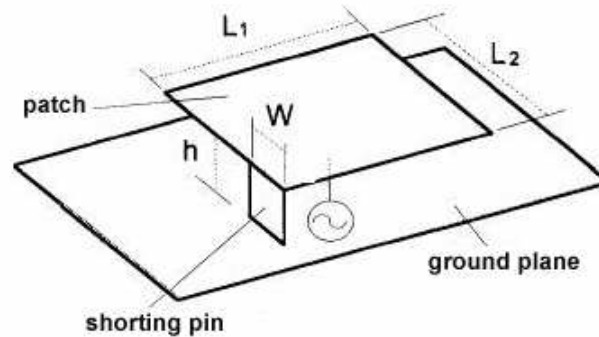


Figure 3.15: Geometry of planar inverted F antenna [22].

Based on the features that define the PIFA antennas, two different studies have been developed. The first one shows the changes in the performance of the antenna when dimensional parameters are modified, and the second one consists of a deep study on how to get a good input impedance matching varying the relative position between the feed pin and the short pin.

The first point to solve is where to put the antenna within the ground plane. From [21] it is stated that to design small and efficient antennas for mobile handsets it is important to utilize the ground plane resonances in an optimal way. Corners of a rectangular ground plane are optimal places for patch type antenna elements, because the electric field of ground plane resonant modes would be maximal in these locations. Therefore, the optimum position of the PIFA in order to achieve an omni-directional far-field pattern and 50Ω impedance matching is close to the edge of the ground plane.

For the first study, based on the equation 3.2, as was done with ILA and IFA antennas, the dimensional parameters L_1 , L_2 , h and W are modified. As the resonance frequency should be 2100 MHz, and setting $h = 10mm$, $W = 0mm$ and $L_2 = 10mm$, the value for the length of the antenna should be around $L_1 = 15.7mm$. From these values, the length and the width of the PIFA antenna are modified. The results showing how the behaviour of the antenna has varied with this two parameters are shown in Figure 3.16. Again, as it is expected, the bigger the antenna, the lower resonance frequency is, and the smaller the antenna, the upper resonance frequency is.

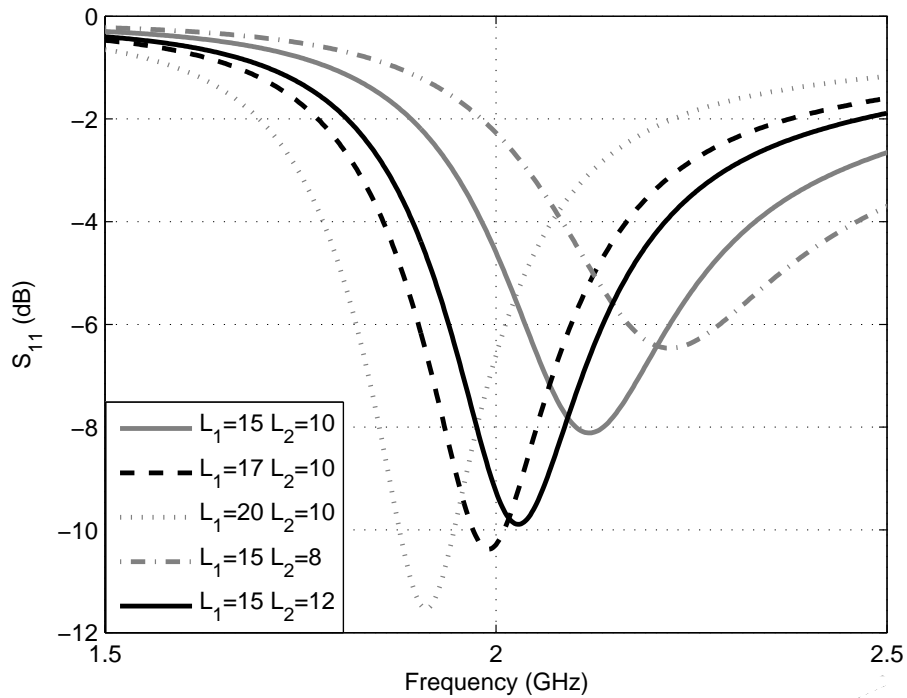


Figure 3.16: Changes in S_{11} in a PIFA antenna when L_1 and L_2 are modified.

Another feature of these antennas is the height, i.e. the distance between the plate and the ground plane. Some values between 10mm and 3mm are tested and the results are represented in Figure 3.17. Based on the graph it can be concluded that by decreasing the distance, a higher resonant frequency can be achieved. This is not strange since, so was the case with L_1 and L_2 , if h is decreased, then the total size of the antenna is decreased too, and the indirect dependency between resonance frequency and PIFA dimensions leads to an increase in the resonance frequency. It is further note that the bandwidth is greater with the reduction of space between the patch antenna and the ground plane.

To compare two different systems it is necessary to have almost the same resonance frequency. Consequently, the system with 5mm thick air substrate is retuned to have the same resonance frequency than the one with 10mm thick air substrate. Figure 3.17 shows that the smaller the thickness, the lower value of S_{11} will be at the resonance frequency. Moreover, the bandwidth in the 5mm thick air substrate is bigger than the other case, having an improvement from 8.7% to 12% .

Changes in the width of the planar element can also affect the determination of the resonance frequency. As seen in Figure 3.18, the resonance frequency decreases with the decrease in short circuit plate width. Otherwise, bandwidth is affected very much by the size of the ground plane. By varying the size of the ground plane, the bandwidth of a PIFA can be adjusted. As shown in Figure 3.19 reducing the ground plane can effectively broaden the bandwidth of the antenna system.

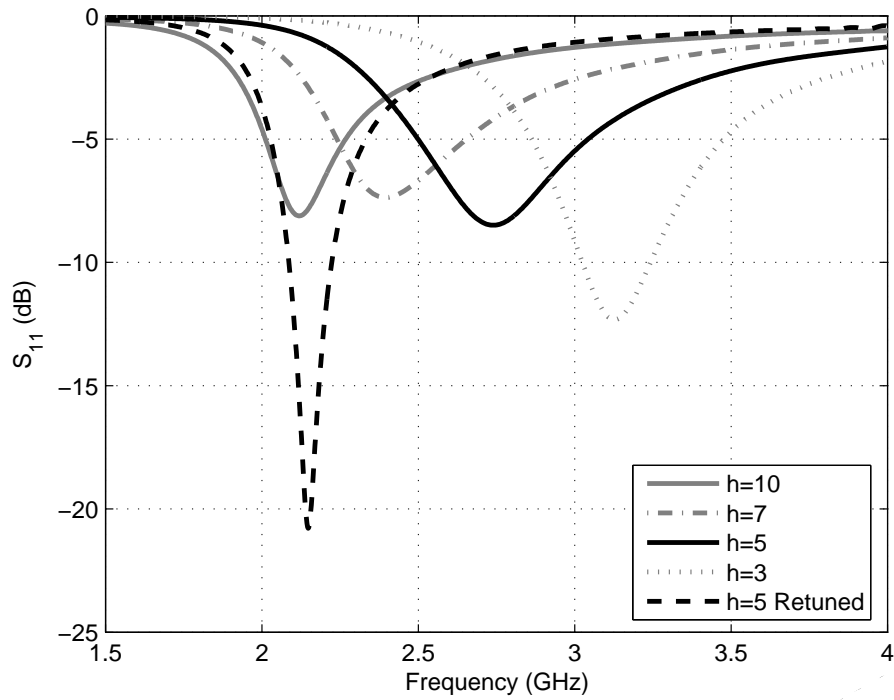


Figure 3.17: Changes in S_{11} in a PIFA antenna when its height h is modified.

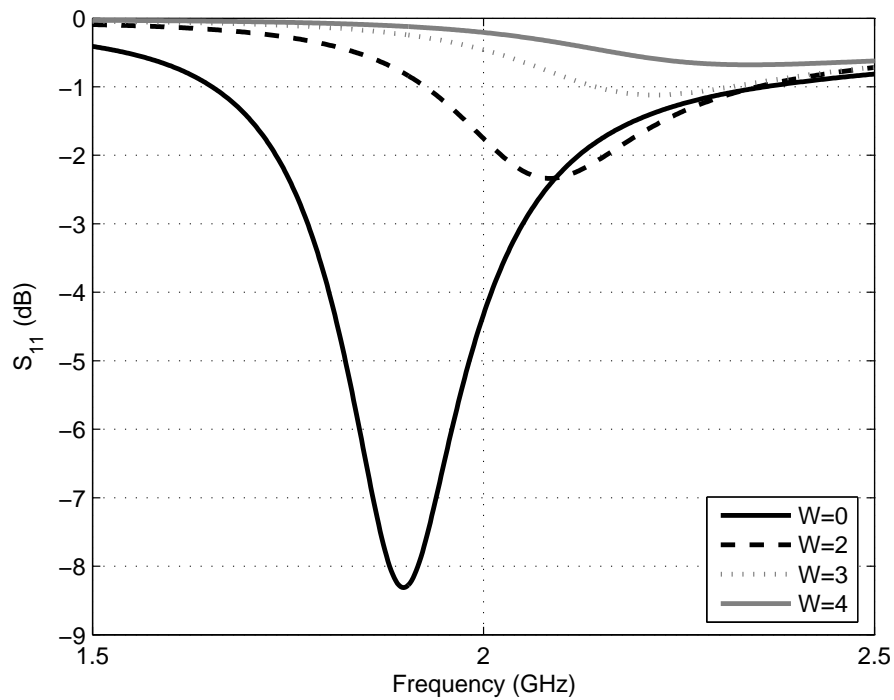


Figure 3.18: Changes in S_{11} in a PIFA antenna when the width of the shorting plate W is modified.

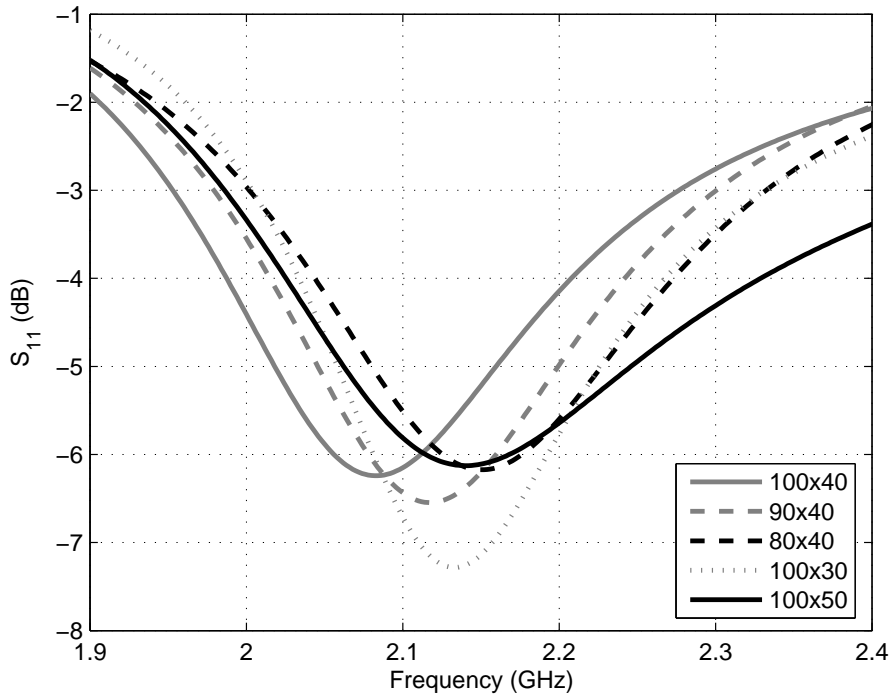


Figure 3.19: Changes in S_{11} in a PIFA antenna when the size of the ground plane is modified.

In the second study the location of the shorting pin and feeding point is optimized in order to achieve the best input impedance matching. So far there is no study of how to get an adequate matching so that what has been done is change the relative position between the feed pin and the short pin and try to draw some conclusions. It is not easy to tune the optimized locations of both pins, thus the procedure that has been used fixes the position of the shorting pin and changes the placement of the feeding pin around it.

To compare different cases it is necessary to introduce the term of mismatch losses. This is a measure of how much the transmitted power is attenuated due to reflection. When the input impedance of the antenna is not equal to the source impedance, part of the incident power is reflected back, so that some losses are introduced into the system. The reflection efficiency or mismatch efficiency, given in equation 3.3, is the ratio of incident power to the power which is finally delivered to the antenna, and gives an idea of how good or bad is the matching.

$$\eta_{mismatch} = 1 - |S_{11}|^2 \quad (3.3)$$

where

$$S_{11} = \frac{Z_{in} - Z_{source}}{Z_{in} + Z_{source}} \quad (3.4)$$

Using equation 3.3, the mismatch efficiency is calculated for all the scenarios of interest. In all cases, the short is positioned in the top edge of the antenna. Firstly, it is located in the upper left corner and then the source is moved to the positions around it. Then, the source is moved $2mm$ to the right and finally, it is moved again $2mm$ to the right. Figure 3.20 depicts, using colours, the values of the mismatch efficiency from the different simulations where the position of the feeding pin was changed. The small blue dot corresponds to the position of the short.

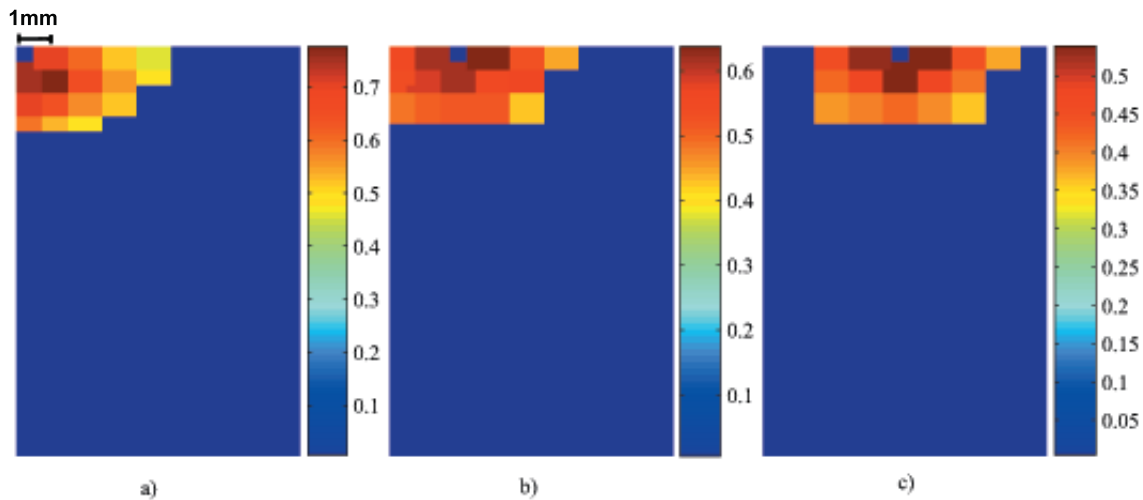


Figure 3.20: Mismatch efficiency depending on the place where the feeding pin and the short pin are placed: a) Short pin in the top left corner b) Short pin $2mm$ to the right from the top left corner c) Short pin $4mm$ to the right from the top left corner

According to the results shown in Figure 3.20 the best location for the short pin is the top left corner of the Printed Circuit Board (PCB) of a typical mobile phone. The feeding pin should be placed next to the short pin, $1mm$ or $2mm$ far from it. The structure with the higher mismatch efficiency has the feeding pin $1mm$ to the right and $1mm$ to the bottom from the corner where the short pin is located. It is a rectangular antenna with a length of $15mm$ and a width of $8mm$. A small patch with length of $1mm$ and width of $2mm$ is also attached in the left bottom corner. It resonates at 2020 MHz and covers all UMTS band I from 1916 MHz to 2178 MHz. The lower value of S_{11} is -13.96 dB and the mismatch efficiency is 0.782 . This antenna is used in the study with two antennas in chapter 4

From all mentioned above, to find a PIFA antenna working at a certain frequency, we must modify the parameters seen to find the desired response. Firstly, it must be calculated the approximate size of the panel using the formula given in equation 3.2. Then, a good input impedance matching can be found by changing the position of the feeding pin and the short pin. At this point, the value of the S_{11} parameter at the resonance frequency is low. If the obtained bandwidth is not the required one, the height of the antenna should be modified. To achieve a narrower bandwidth, the distance between the ground plane and the PIFA antenna should be longer. To achieve a wider bandwidth, the distance should be shorter. Normally, when some parameter changes, the resonance frequency shifts. Modifying the width and length of the antenna, the resonance frequency can be placed at the working frequency.

3.2 Reception and transmission antennas

As it already mentioned at the beginning of the chapter, in communications systems is very common to separate transmission from reception to avoid problems due to interferences between signals. UMTS band *I* was launched in the core band (1920-1980 MHz/2110-2170 MHz). Based on the knowledge acquired previously, in this section antennas that covers the uplink and the downlink of UMTS 2100 are designed.

In the case of ILA and IFA antennas, to cover both links, they must be designed to have a narrower bandwidth. Table 3.1 shows the lengths and width of the arms of the transmission and reception ILA antennas. Otherwise, Table 3.2 provides the lengths and widths of the arms of the IFA antennas and the distance between the source and short arms. The S_{11} parameter along the frequency is depicted in Figure 3.21.

ILA	$H(mm)$	$V(mm)$	$W_H(mm)$	$W_V(mm)$
Uplink	24	7	1	1
Downlink	26	10	1	1

Table 3.1: Dimensions of ILA antennas that cover the downlink and the uplink

IFA	$H(mm)$	$V(mm)$	$W_H(mm)$	$W_V(mm)$	$S(mm)$
Uplink	29	5	1	1	1
Downlink	26	5	1	1	1

Table 3.2: Dimensions of IFA antennas that cover the downlink and the uplink

As can be seen in Figure 3.21 the input impedance matching is better in IFA antennas than in ILA antennas. It is easier to obtain narrower bandwidth with IFA antennas, because the short arm gives to the designer more possibilities to obtain the desirable behaviour of the antenna [26].

For PIFA antennas, the new required bandwidth is narrower and thus the total volume smaller, i.e. the distance between the antenna and the ground plane has to be smaller. By reducing the height of the antenna, the resonance frequency shifted to upper frequencies. To locate it at the desired frequency, the antenna dimensions are increased. Two different PIFAs, with a $3mm$ thick air substrate, are designed. The one supposed to cover the downlink is a $20mm$ length by $10mm$ width. Its bandwidth includes all frequencies from 2051 MHz to 2236 MHz, reaching a S_{11} value of $-10.27dB$ at 2132 MHz. For the uplink, as the resonance frequency has to be lower, the surface of the patch should be larger, specifically its length is $23mm$ and its width $10mm$. On this occasion, the value of S_{11} at the resonance frequency (1960 MHz) is -8.403 and the operating bandwidth includes 2907-2023 MHz. The S_{11} parameter along the frequency is depicted in Figure 3.21. As intended, the bandwidths of the antennas are spaced so there is less possibility of interference.

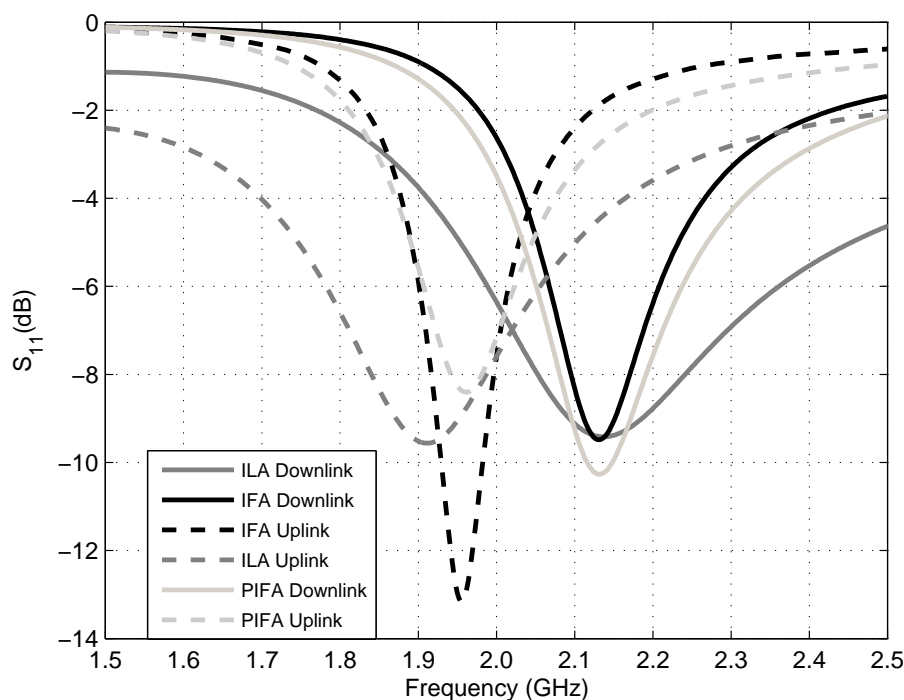


Figure 3.21: S_{11} of ILA and IFA antennas for transmission(Uplink) and reception(Downlink) for UMTS Band *I*

3.3 UMTS band *I*, band *II* and band *V* antennas

This section aims to make a comparison between the size and behaviour of different antennas designed for the most used bands in UMTS. These are band *I* (2100 MHz), band *II* (1900 MHz) and band *V* (850 MHz). The main concern when selecting one antenna instead of another is the matching that has to be the lower as possible and at least lower than $-6dB$ in all the bandwidth. In Table 3.3, Table 3.4 and Table 3.5 the dimensions of the antennas are provided where the letters used are the same as those represented in Figure 3.1 for ILA antenna, in Figure 3.5 for IFA antenna and in 3.15 for PIFA antenna.

ILA	$H(mm)$	$V(mm)$	$W_H(mm)$	$W_V(mm)$
Band <i>I</i>	24	9	1	1
Band <i>II</i>	26	10	1	1
Band <i>V</i>	87	12	1	1

Table 3.3: Length and width of the components of the ILA for each band

Figure 3.22, Figure 3.23 and Figure 3.24 represent the input impedance matching of the IFA and ILA antennas for all bands respectively.

IFA	$H(mm)$	$V(mm)$	$W_H(mm)$	$W_V(mm)$	$S(mm)$
Band I	24	8	2	1	6
Band II	31	5	1	1	4
Band V	89	9	3	2	3

Table 3.4: Length and width of the components of the IFA for for each band

PIFA	$L_1(mm)$	$L_2(mm)$	$h(mm)$	$W(mm)$
Band I	15	8	10	1
Band II	22	10	5	1
Band V	27	40	10	1

Table 3.5: PIFA dimensions for each band

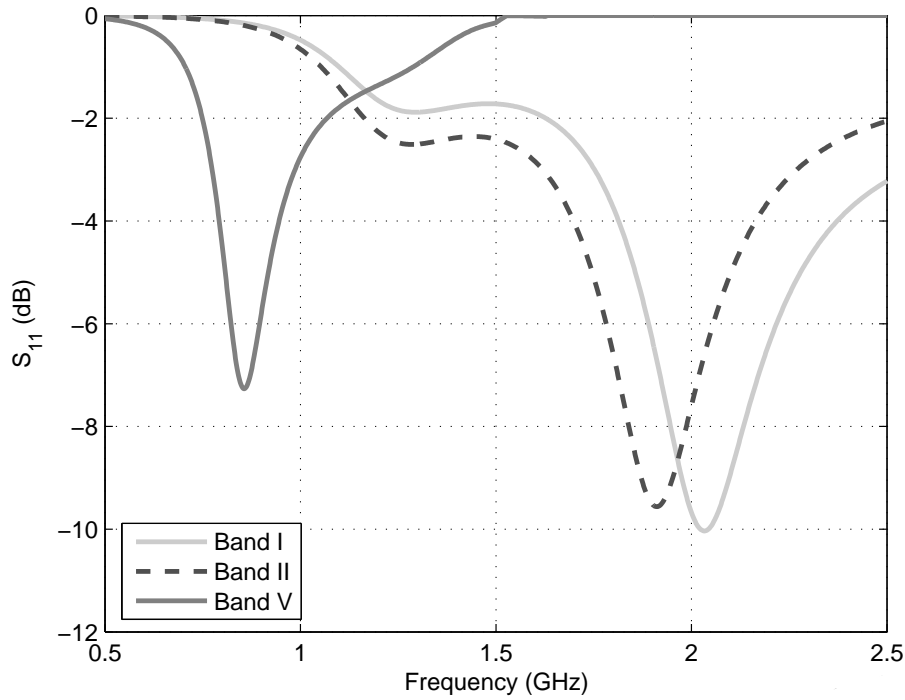


Figure 3.22: S_{11} of designed ILA antennas for Band I, II and V

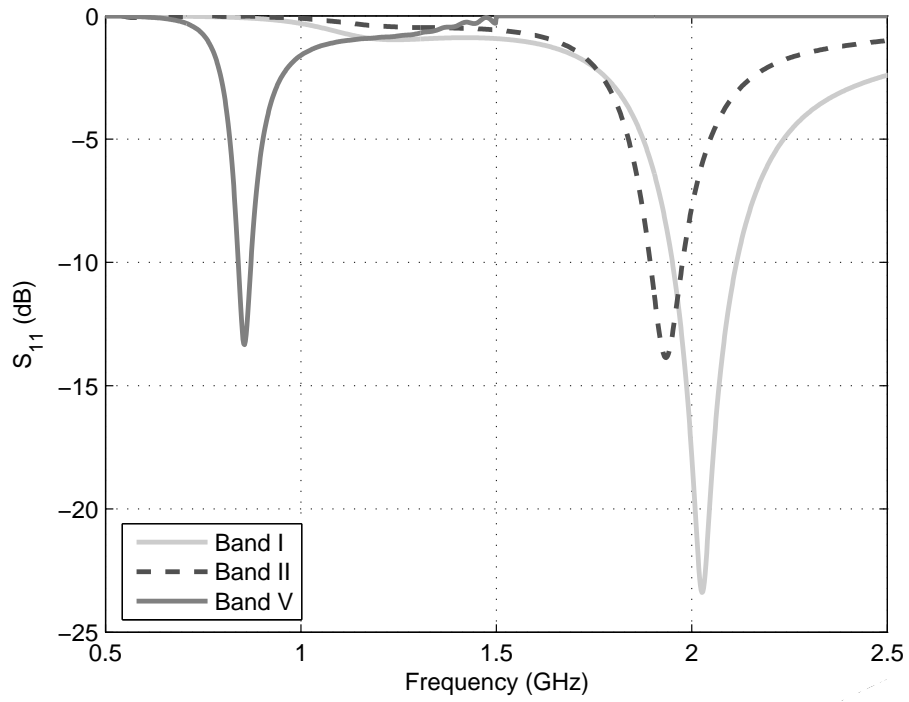


Figure 3.23: S_{11} of designed IFA antennas for Band I, II and V

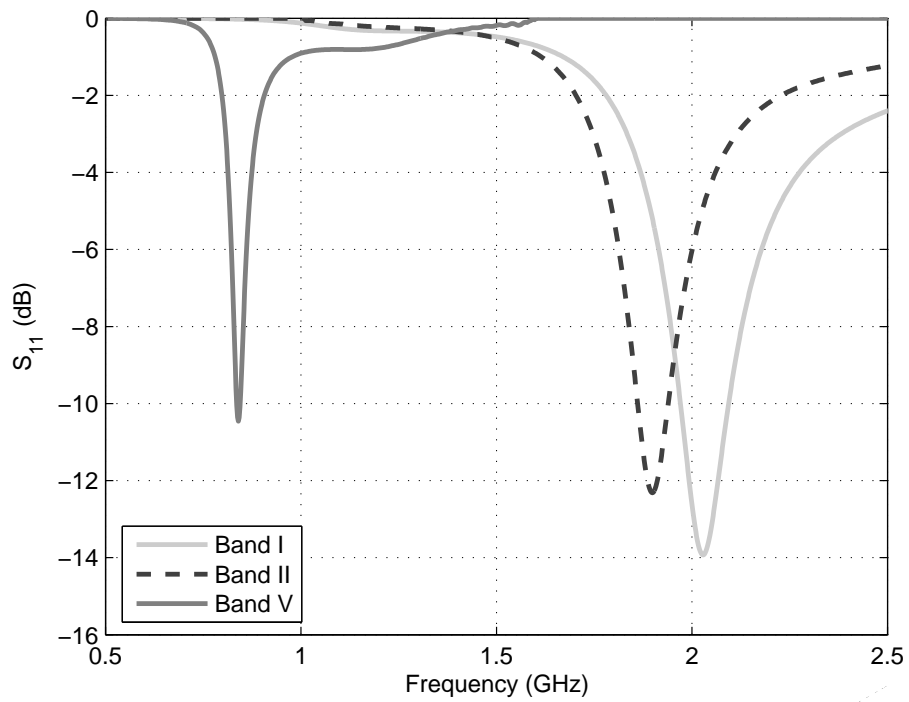


Figure 3.24: S_{11} of designed PIFA antennas for Band I, II and V

Study of dual antenna systems

Nowadays, the trend is to multiply the number of the radiating elements on a mobile handset to increase the probability to receive a good signal. This increase of the needs for wireless communication quality, has induced the development of multi-antenna systems like diversity and multiple input multiple output (MIMO), that are explained in appendix D. However, the proximal placement of the antennas causes an increase of the insertion loss between their feeding ports and therefore degrades the overall diversity performance.

Also the enclosure in which the antennas are mounted affects their performance, because they radiate electromagnetic waves that interact with resonant and absorbing materials nearby [17]. This interaction can reduce the efficiency of an antenna. The causes are some reflections due to the interference between directly radiated antenna waves and waves reradiated by different parts of the enclosure.

In the “transmit mode” coupling definition [15], an excitation source is placed at the feed of one antenna, and the other antenna is terminated in a load. Coupling between the two antennas is then calculated by

$$C = \frac{P_L}{P_D} \quad (4.1)$$

where

- C : Mutual coupling between two antennas
- P_D : power radiated by the excited antenna
- P_L : power delivered to the load of the un-excited antenna.

Also the S-parameters are related to the transmit-mode coupling calculation by

$$|S_{21}|^2 = (1 - |S_{11}|^2) \cdot C \quad (4.2)$$

The purpose of this chapter is therefore the study of mutual coupling and isolation of different systems consisting of two antennas. Following the same scheme of chapter 3, some simulations of a ground plane with two antennas that cover all UMTS band I are made. Then the same procedure is repeated for two antennas designed one for transmission and one for reception. Finally, it is also analyzed the mutual coupling and isolation for another class of mobile terminals called clamshells.

4.1 Study based on the antenna features

The main problem in MIMO systems, is to find the right place to put the antennas. In chapter 3 concerning single antennas, it was stated that the corners of a rectangular ground plane are optimal places for patch type antenna elements, because the electric field of ground plane resonant modes would be maximal in these locations. Thereupon there are three possibilities to situate the antennas as illustrated in Figure 4.1: at the corners in the top or bottom of the ground plane, at the corners in the left or right side of the ground plane and one in a corner of the top of the ground plane and the other one in the opposite corner in the bottom. Simulations of the different alternatives for placing the PIFA antennas have been made and the results are presented in Figure 4.2.

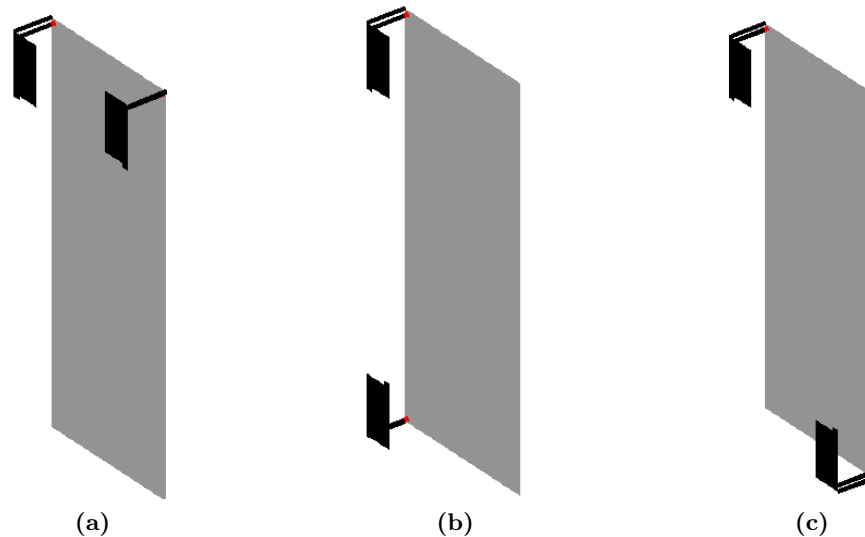


Figure 4.1: Different possibilities to locate two antennas in a ground plane. a) Both in the top. b) Both in the left side. c) One in the opposite corner to the other.

Once it is known where to place the radiating elements, some structures with two antennas are introduced. As it was already mentioned, the antennas used for the simulations are ILAs, IFAs and PIFAs. Figure 4.3 shows the input impedance matching and the mutual coupling of structures with the same type of antennas placed in opposite corners, i.e. two ILAs, two IFAs and two PIFAs.

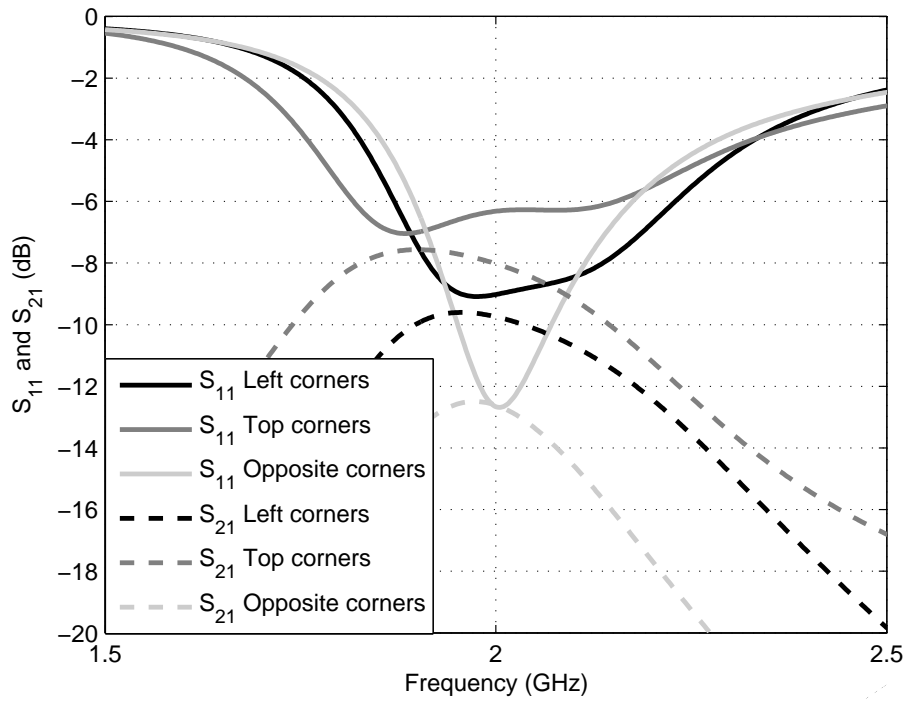


Figure 4.2: S_{11} and S_{21} in a system of two PIFA antennas depending on the disposition of such antennas

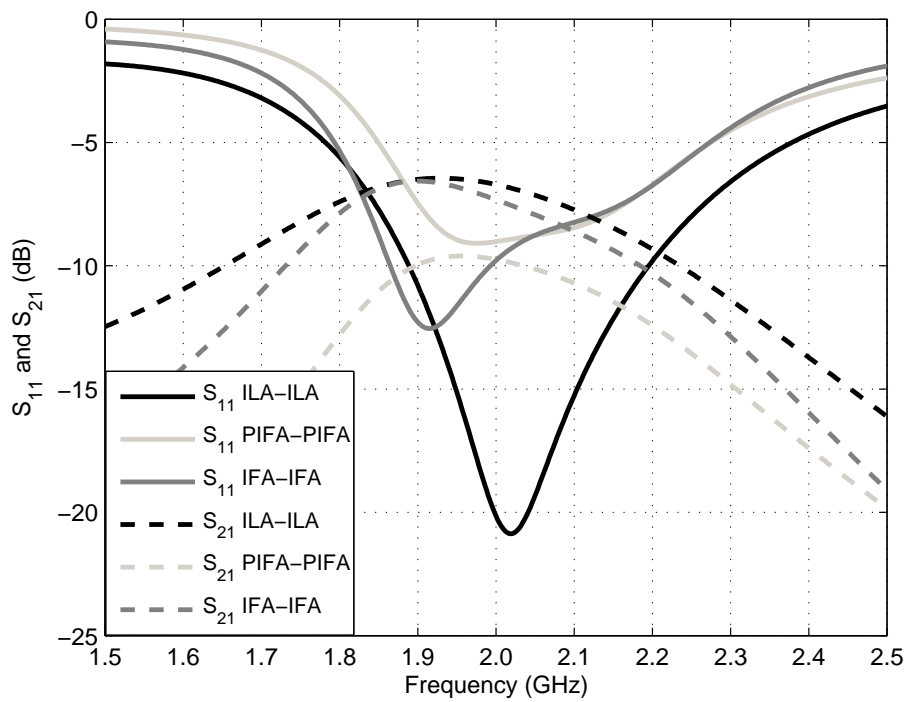


Figure 4.3: S_{11} and S_{21} of two equal antennas systems. At figure are represented the response of ILA, IFA and PIFA two antennas system.

Figure 4.4 the matching and mutual coupling of the antennas in a structures with two different antennas, in this case there are shows the structures with all the possible combinations between ILA, IFA and PIFA antennas.

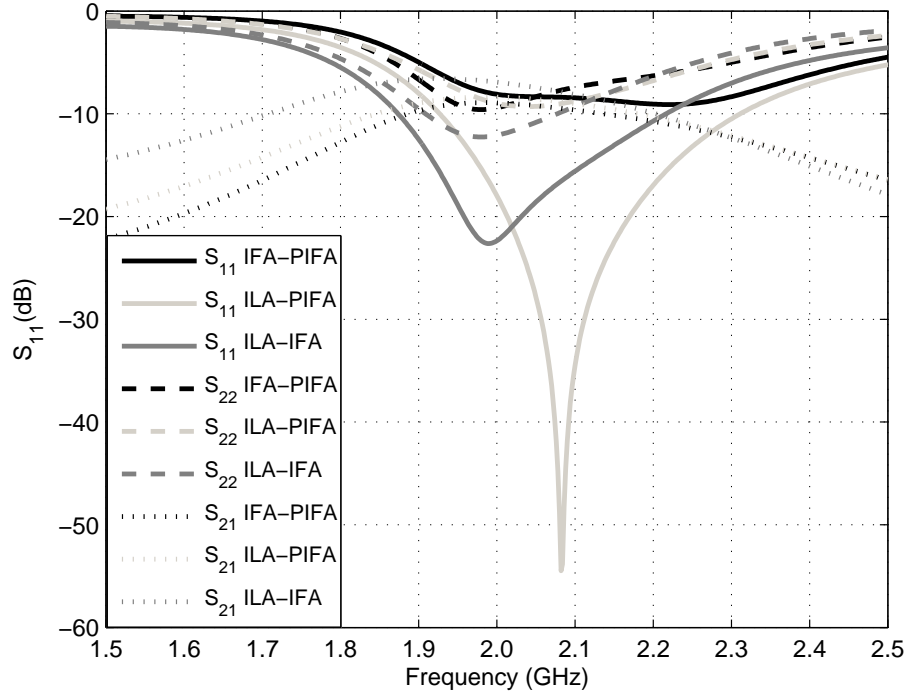


Figure 4.4: S_{11} and S_{21} in a system of two antennas. In this case both antennas of each system are different. ILA, IFA and PIFA antennas are used for these simulations

4.2 Uplink and Downlink antennas

The study undertaken in Chapter 3, which stated that it is very common to separate transmission from reception to avoid problems due to interferences between signals. For all types of antennas, ILA, IFA and PIFA some structures are designed. They simulate mobile terminals with an antenna for transmission that covers the uplink of the UMTS band *I* (1920-1980 MHz), and one for reception that covers the downlink of the UMTS band *I* (2110-2170 MHz).

Comparing the results given in Figure 4.5, IFA and PIFA are more appropriate to design antennas for transmission and reception, due to it is easier to obtain a narrower bandwidth. The best isolation is achieved for the case of the PIFA antennas.

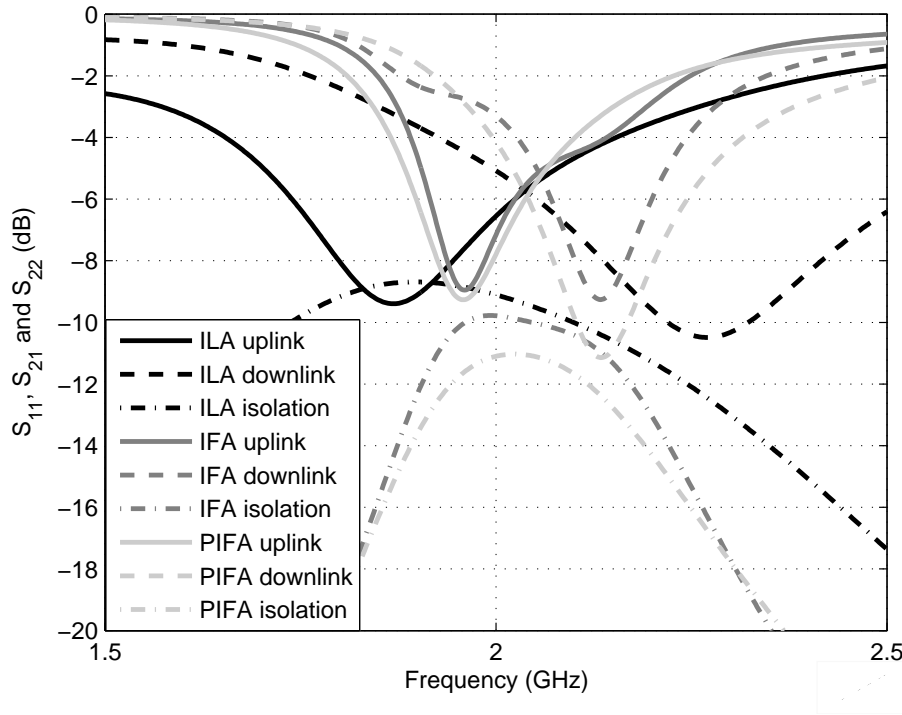


Figure 4.5: Input impedance matching and isolation of ILA, IFA and PIFA antennas designed for transmission and reception.

4.3 Antennas for Clamshell handsets

A clamshell mobile is a mobile phone form factor where the phone is divided into two equal halves with a hinge connecting the halves, enabling users to basically fold the phone in half to close when it is not in use. This type of mobile phone usually has the buttons on the bottom half and the display and speaker on the top half. Some clamshell mobiles may also have a small display on the outside, so when the phone is folded you can view connection details, incoming calls and the date and time without opening the phone. It is also called a flip phone. Figure 3.10 shows one of many mobile terminals on the market.

For the simulations of a clamshell phone, it is assumed that the typical Printed Circuit Board (PCB) is 200mm long and 40mm wide. The same type of antennas are located at opposite corners. Therefore, three different simulation are depicted in Figure 4.6, one for each type of antenna. Of course, the fact of placing the antennas on a larger ground plane implies a change in their behaviour. It is necessary to retune the antenna.

The ILA antenna that gives good results working in a clamshell has a vertical arm of 10mm long, and the horizontal one of 25mm . Both widths are 1mm . The IFA antenna, has two vertical wires, the source and the short, with a length of 11mm and a width of 1mm . The vertical arm is also 1mm wide, except the part between the short and the source that is 2mm wide. Finally, the PIFA antenna is 20mm long and 9mm wide, with a 5mm thick air substrate between the antenna and the ground plane.

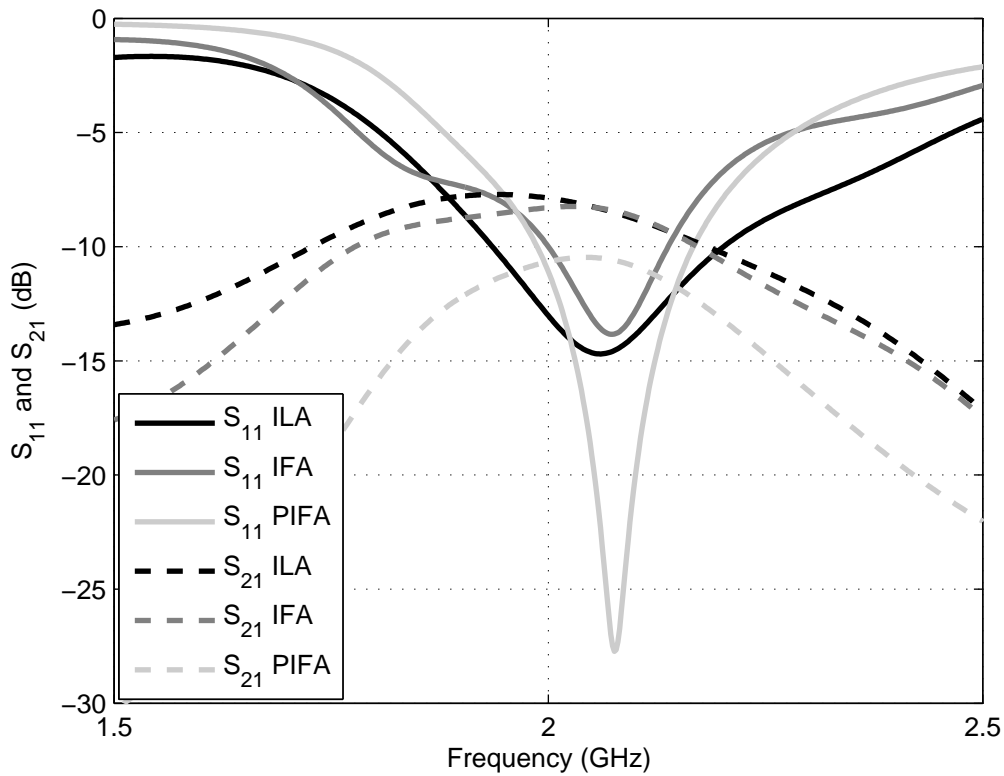


Figure 4.6: S-parameters of a Clamshell printed circuit board with two ILA, two IFA or two PIFA antennas.

Based on the results provided in Figure 4.6, anew the IFA and PIFA antennas have a narrower bandwidth that conforms to the bandwidth of UMTS technology band *I*. A better input impedance matching is attained. Moreover, as it was expected, the fact of having a larger ground plane is an improvement in the isolation between antennas.

Techniques to improve isolation

Sufficient isolation between antennas is important in diversity and MIMO systems. The coupling between antennas decreases their efficiencies as part of the power that would normally be radiated is captured by the other antenna.

For many years, numerous studies have been done to find techniques that reduce the mutual coupling and increase the isolation between antennas. To achieve the reduction of the S_{21} parameter, the main idea consists in introducing some additional coupling path between the radiators. Several techniques have been reported for high isolation characteristics by inserting a band stop matching circuit [13], placing a neutralizing line between the two antennas [2], two identical antennas that have current paths orthogonal to each other [16], using electromagnetic band gap structures (EBG) [11], T-shaped and dual inverted L-shaped ground branches [29], etc.

In this project, two different techniques have been investigated:

- Place dielectric substrates between the two antennas.
- Use a defected ground plane (DGP).

To compare two different systems it is necessary to introduce the definition of the total efficiency. In a multi-antenna system, the total efficiency η_T is the relation between the power delivered by the source into the system and the power that finally is radiated after the coupling with other antennas. The efficiency of the antennas in their environment is reduced by all losses suffered by it, including: ohmic losses, mismatch losses, feedline transmission losses, edge power losses, etc.

The total efficiency can be defined as the product of radiation efficiency, reflection efficiency and coupling efficiency (equation 5.1). The Radiation efficiency η_r is the relation between the radiated power and the power delivered to the antenna and it is related with the antenna impedance. The reflection efficiency η_{ref} is the relation between the power that arrives to the antenna and the power which is finally delivered to the antenna. It depends on the reflection coefficient. The coupling efficiency η_c in a system with two antennas is the relation between the radiated power from one antenna and the power which is absorbed by the other antenna.

$$\eta_T = \eta_r \cdot \eta_{ref} \cdot \eta_c \quad (5.1)$$

The total efficiency can also be calculated from the scattering parameters, as shown in equation 5.2:

$$\eta_T = \eta_r \cdot (1 - |S_{11}|^2 - |S_{21}|^2) \quad (5.2)$$

When the antennas placed in the printed circuit board are not designed to resonate at the same frequency, e.g. in a transmission and reception system, another statistic should be taken into consideration, i.e. the envelope correlation. The correlation between the signals from two antennas in a scattering environment is an important parameter for multiple-input–multiple-output (MIMO) systems. It can be measured directly or calculated from the full-sphere radiation patterns [24]. Both methods require special measurement equipments. For isotropic signal environments the correlation can be obtain from the S-parameters of the antennas (equation 5.3), i.e. the port reflection coefficients S_{11} and S_{22} of the two antennas, and the coupling $S_{21} = S_{12}$.

$$\rho_e = \frac{|S_{11}^* S_{12} + S_{21}^* S_{22}|}{(1 - |S_{11}|^2 - |S_{21}|^2) \cdot (1 - |S_{22}|^2 - |S_{12}|^2)} \quad (5.3)$$

Considering all the above, the study to improve the isolation between antennas using the mentioned techniques is presented.

5.1 Dielectric Walls

Dielectric Materials are electrical insulators or materials in which an electric field can be sustained with a minimal dissipation of power. They are characterized by the dielectric permittivity (ϵ), that is a measure of how an electric field affects, and is affected by, a dielectric medium. It is determined by the ability of a material to polarize in response to the field [19].

For a long time dielectric substrates have been used as isolators. For instance it is easy to find them in coaxial cables between the centre core and the metallic shield. Consequently two dielectric walls with the following features (see Figure 5.1) are placed on the ground plane in order to improve the isolation:

- Length (L): 40 mm.
- Height (H): 10 mm.
- Width (W): 2 mm.
- Permittivity (ϵ): 50 F/m.
- Conductivity (σ): 0 S · m⁻¹.

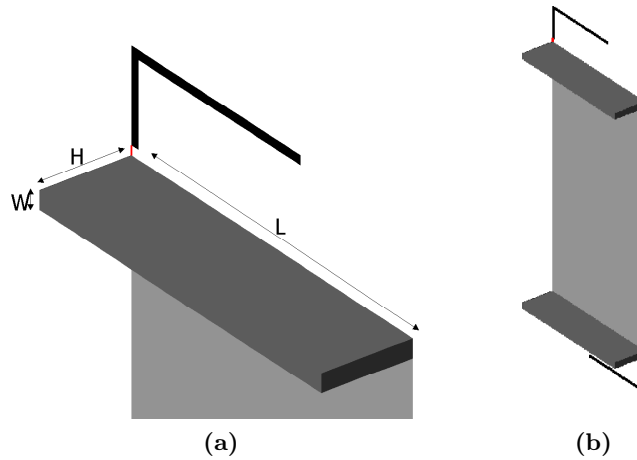


Figure 5.1: (a) Dielectric wall features. (b) Dielectric walls placed on the printed circuit board

First of all, the position of the dielectric walls on the ground plane is modified. Initially, two dielectrics are placed in the center of the ground plane, and then they are moved closer to the antennas in steps of 10 mm . till a distance of 30 mm . from the center of the ground plane is reached. Figure 5.2 shows how the matching and the mutual coupling change depending on the position. As can be seen, the position of the dielectric walls affects not only the isolation between antennas, but also the resonance frequency. For this reason, once the dielectric wall is placed on the ground plane the antenna has to be retuned, because its resonance frequency shifted to lower frequencies. The change experienced by the resonance frequency depends on the features of the dielectric wall. These are the permittivity and the size of the wall and its position on the ground plane. However, when the dielectric approaches to the antenna, there is a slight improvement in the isolation.

Other feature to change is the width of the dielectric walls. Figure 5.3 shows the input impedance matching and the isolation of two different systems that consist of two dielectric walls located 40 mm . from the center of the ground plane. One of them has a 2 mm . wide dielectric and the other one 3 mm .. It is important to note that both structures have been retuned to 2100 MHz to compare them. As it was already mentioned, the radiation efficiency is useful to compare different systems. Figure 5.4 provides the radiation efficiency of the structure without dielectric, and with 2 mm . and 3 mm . wide dielectrics.

When the dielectric is wider than 3 mm the shift to low frequencies is bigger and is not possible to retune to high frequencies without losing bandwidth. In this cases, it is impossible to cover all the band.

Based on the results, this dielectric walls do not improve the total efficiency of the system. Although with dielectrics lower values of S_{21} are achieved, also the input impedance matching S_{11} is worse, thereby, as the total efficiency depends on both parameters, it can be worse.

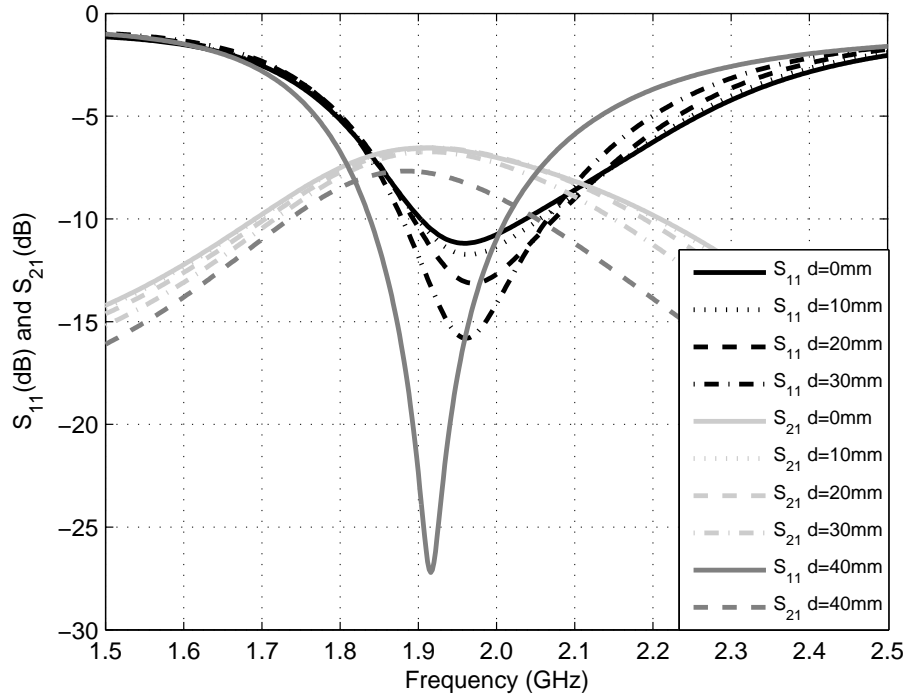


Figure 5.2: Changes in S_{11} and S_{21} in a system with two ILA antennas when the position of the dielectric wall changes along the ground plane.

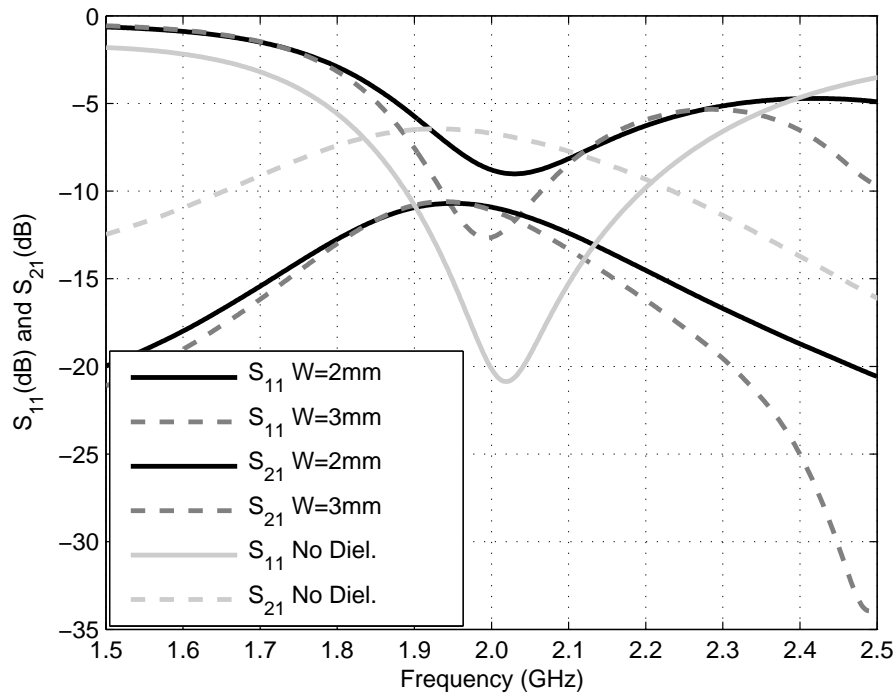


Figure 5.3: S_{11} and S_{21} in a two ILA antenna system depending on the width of the dielectric walls.

Otherwise, the permittivity of the dielectric also makes the resonance frequency change. The higher value the permittivity, the bigger frequency shift to lower values is and the deeper and narrower the S_{11} is. Figure 5.5 shows S_{11} and S_{21} of a two ILA antennas structure with two dielectric walls of $2mm$. width, placed $40mm$. from the centre in both sides of the ground plane. Values of $20 F/m$, $50 F/m$ and $80 F/m$ are used for the permittivity. From the results, except the case of $\epsilon = 80$ that is a strange response, the isolation do not change a lot with changes in the permittivity of the dielectrics.

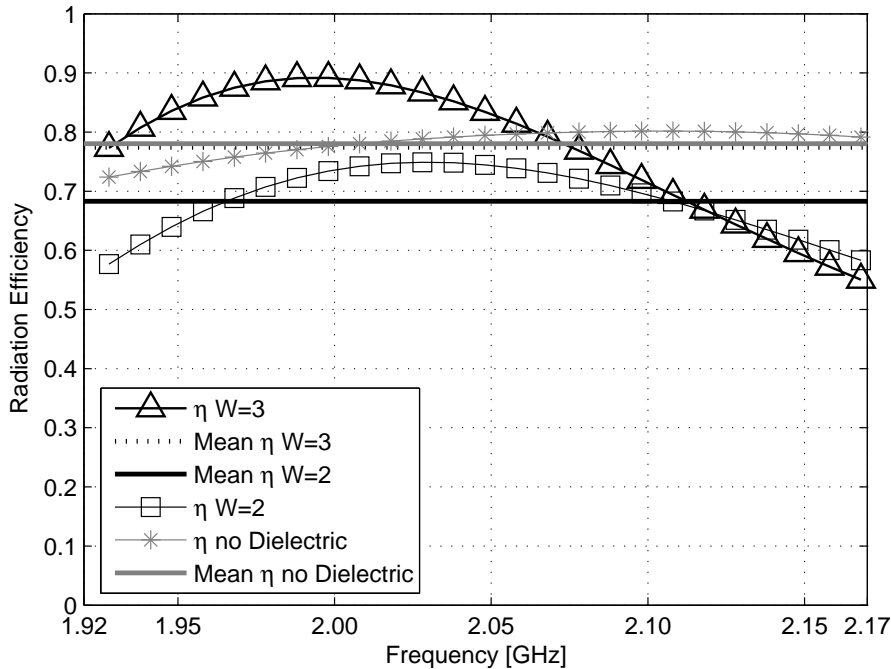


Figure 5.4: Total Efficiency of a two ILA antenna system depending on the width of the dielectric walls.

In the following part, it is made comparisons of some structures designed from all the possible combinations between the three types of antennas (ILA, IFA and PIFA). The purpose is to find a satisfactory system that improves the isolation. The criterion for determining which structure is better, is the radiation efficiency. Figure 5.6 shows the results of the structures with dielectric walls and two equal antennas. The total efficiency of these structures is depicted in Figure 5.7.

As seen in the graph, except for ILA antennas, due to the dielectric walls, the current flows from one side of the ground plane to the other side are substantially reduced and this effectively helps to reduce the mutual coupling between the two antennas. The most relevant case is the IFA antennas which achieve an improvement of 8% in the total efficiency.

The same is repeated for structures with dielectric walls and two different antennas, selected from ILA, IFA and PIFA. Figure 5.8 shows the input impedance matching and the isolation of all the different cases.

The next systems where the dielectric walls are tested are those where the transmission and reception are designed separately. In this case, only two ILA and two IFA antennas are placed on the printed circuit board. Figure 5.9 illustrates the differences between the input impedance

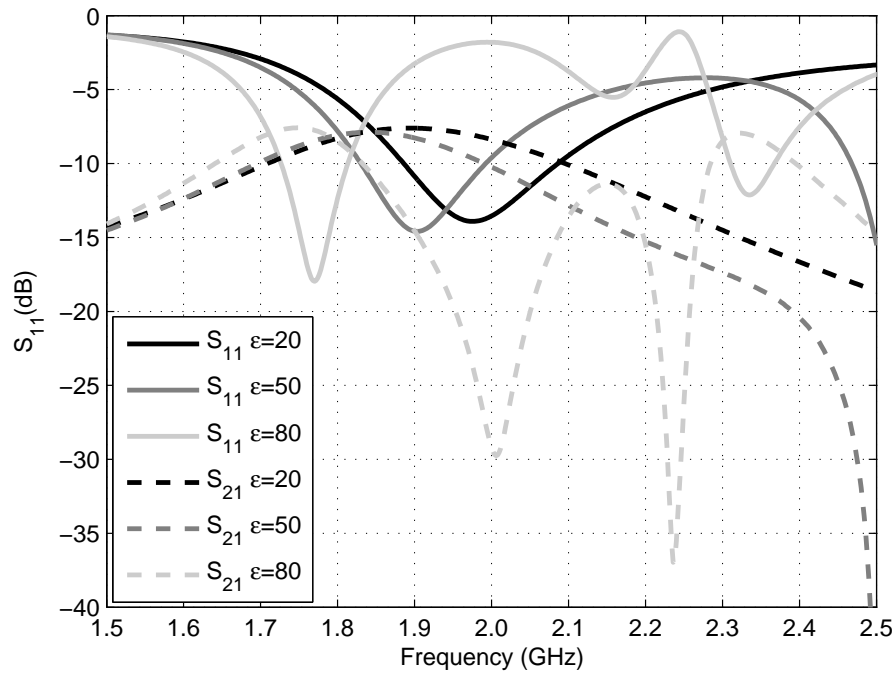


Figure 5.5: S_{11} and S_{21} in a two ILA antenna system depending on the permittivity of the dielectric walls.

matching and the isolation of this two structures. Analyzing the results, it is found that by applying the proposed dielectric walls, the isolation between the antennas can be improved 2.6 *dB*. Even the input impedance matching of the downlink antenna is better. Moreover, Figure 5.10 shows the same procedure for IFA antennas. The results are similar, it is achieved an improvement of almost 4 *dB*, but in this case, the uplink is the one who improves its value.

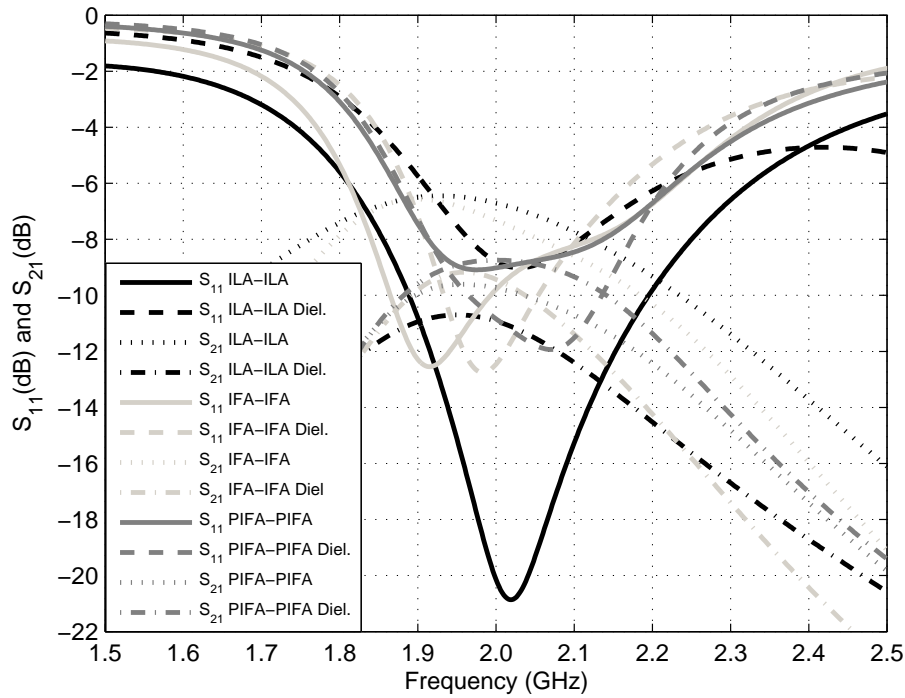


Figure 5.6: S_{11} and S_{21} of structures consisting of two equal antennas and two dielectric walls, compare to systems with the same antennas, but without dielectric walls.

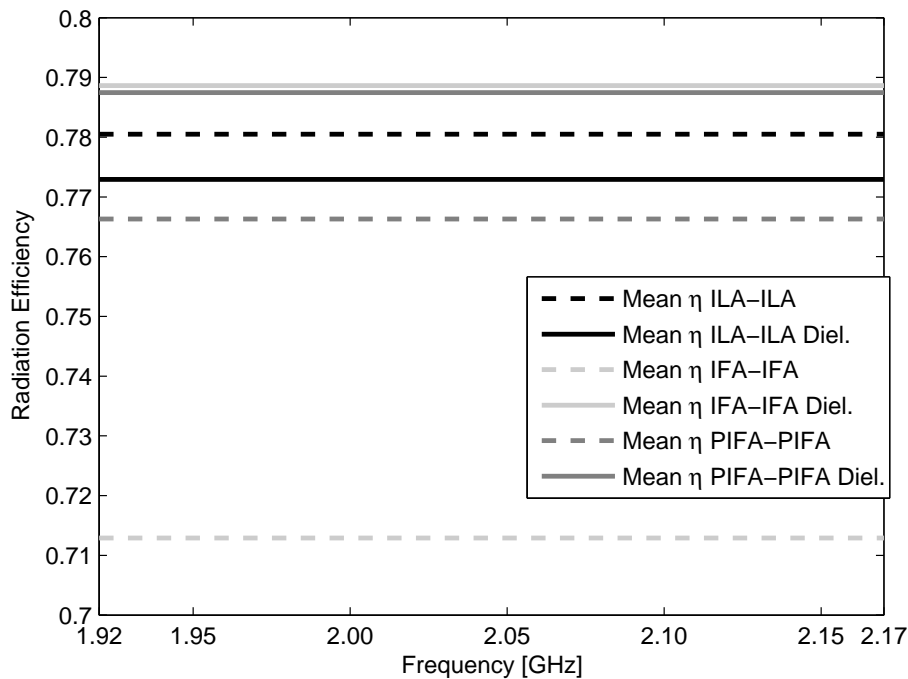


Figure 5.7: Total efficiency of structures consisting of two equal antennas and two dielectric walls, compare to systems with the same antennas, but without dielectric walls.

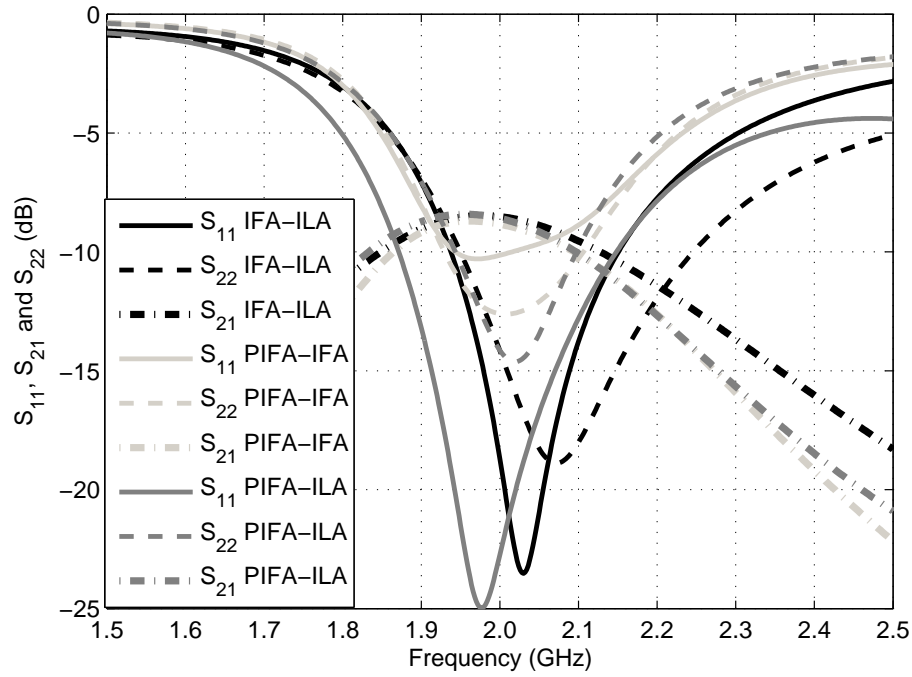


Figure 5.8: S_{11} , S_{21} and S_{22} of structures consisting of two different antennas and two dielectric walls, compare to systems without dielectric walls.

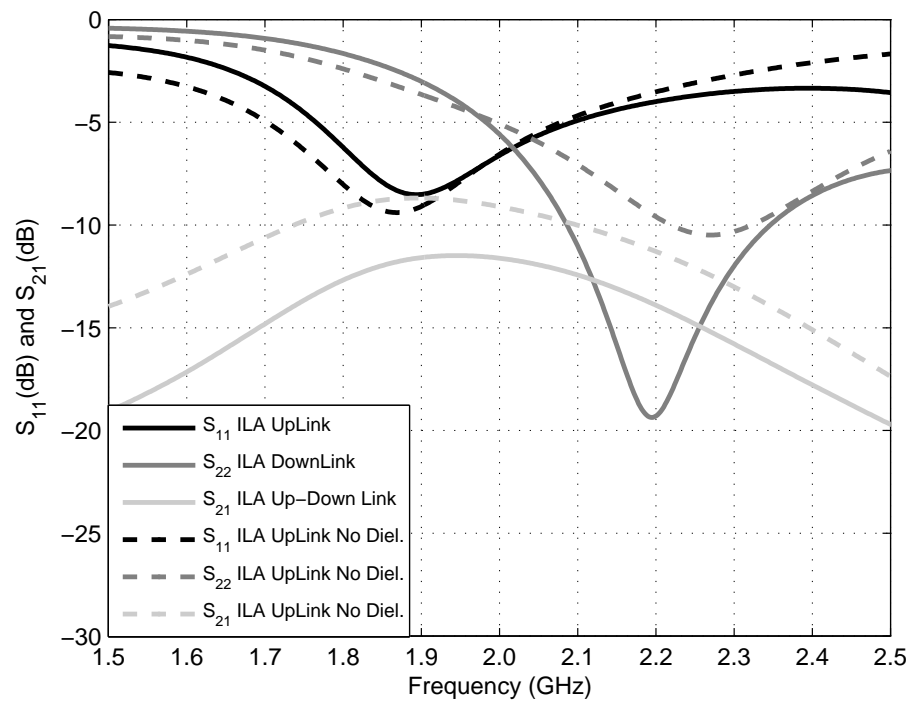


Figure 5.9: S_{11} and S_{21} of structure with two ILA antennas and two dielectric walls, compare to the case without dielectric walls. Each antenna is designed to cover one link of the UMTS band *I*.

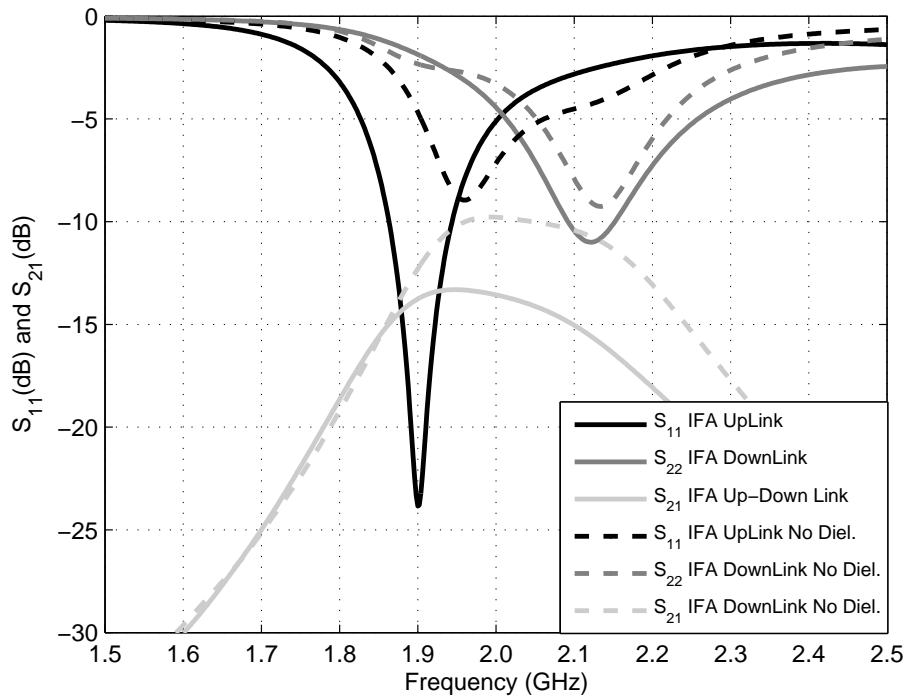


Figure 5.10: S_{11} and S_{21} of structure with two IFA antennas and two dielectric walls, compare to the case without dielectric walls. Each antenna is designed to cover one link of the UMTS band I.

The total efficiency of all the structures presented above is depicted in Figure 5.11. This parameter helps to determine which structure is better because it takes into account both the input impedance matching and the isolation. As the antennas are designed to cover only the uplink or the downlink, the mean value of the total efficiency is calculated only inside this bands, i.e. between 1920 MHz and 1980 MHz for the uplink and between 2110 MHz and 2170 MHz for the downlink. As it was expected, the total efficiency in all the cases is higher, reaching an increase of 15% for the case of an iLA antenna working in the uplink.

Finally, clamshell phones are the last scenario to work with dielectric walls. As it was already mentioned in previous chapters, this kind of structures have a longer ground plane, with dimensions of 200mm long and 40mm wide. Figure 5.12 gives a comparison of the S_{11} and S_{21} parameters between ILA and IFA antennas. Once again the isolation is improved, as evidenced by the representation of the total efficiency in Figure 5.13 where it is shown that both ILA and IFA structures enhance the radiation efficiency when dielectric walls are used.

5.2 Defected Ground Plane DGP

The purpose of using a DGP as a technique to improve the isolation between two antennas is to make use of the ground plane itself to provide a filter effect. This effect suppresses the surface waves, and thus it provides a lower mutual coupling between the antennas [10]. This can be done with a combination of capacitance and inductance effects by means of several slits etched in the middle of the printed circuit board. A deeply study of a DGP with slits in both sides of the

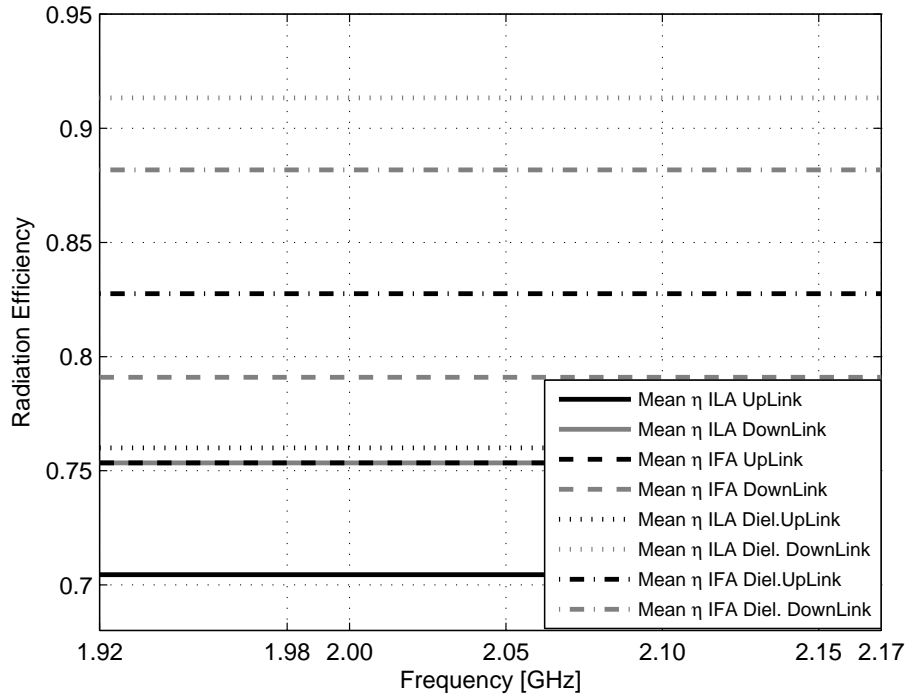


Figure 5.11: Radiation Efficiency of structure with two antennas with dielectric wall. Comparative between ILA-ILA and IFA-IFA where each antenna is tuned only for UpLink(1920MHz-1980MHz) or DownLink(2110MHz-2170MHz).

ground plane is presented. Two equal PIFA antennas are the radiated elements and the location and dimension of the slits are described by the following parameters, provided in Figure 5.14:

- N : Number of slits in each side of the ground plane.
- w : width of the slits [mm].
- s : Distance between slits from the same side of the ground plane [mm].
- c : Distance between slits from different sides of the ground plane [mm].

The slits on one side of the ground plane are located in the same position of the slits in the other side. The number of slits on either side is the first parameter to be modified. The results of the simulations for $N = 0, 1, 3, 5$ are provided in Figure 5.15. In all cases, $w = 1mm$, $s = 1mm$ and $c = 2mm$. The effects on the isolation improving are slight for different numbers of slits. The advantage is that having almost the same mutual coupling between antennas, there is a better input impedance matching if the number of slits on both sides of the ground plane increases.

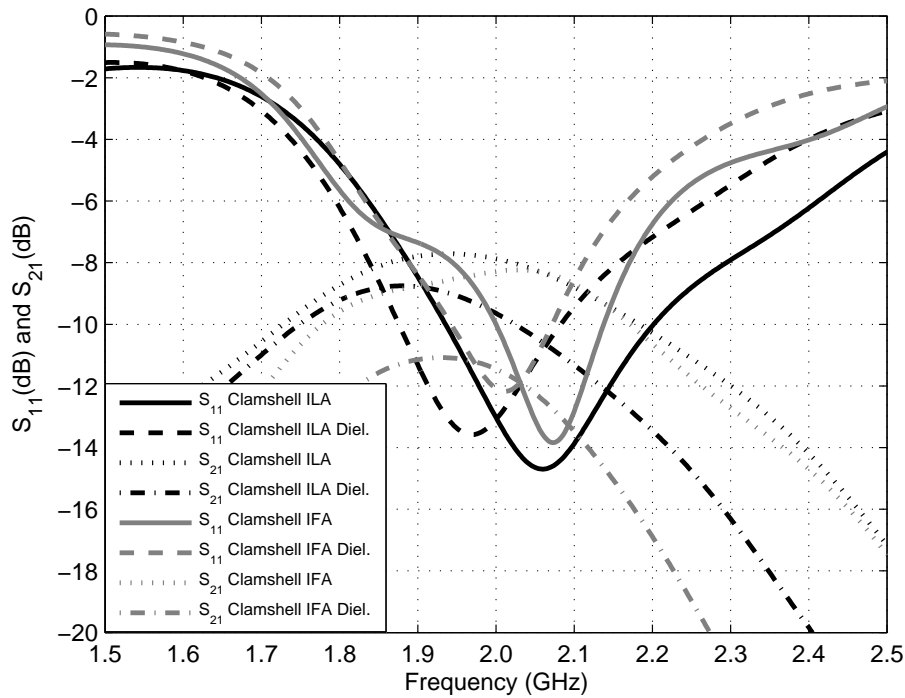


Figure 5.12: S_{11} and S_{21} in a clamshell system with two antennas and two dielectric walls compare to systems with the same antennas, but without dielectric walls.

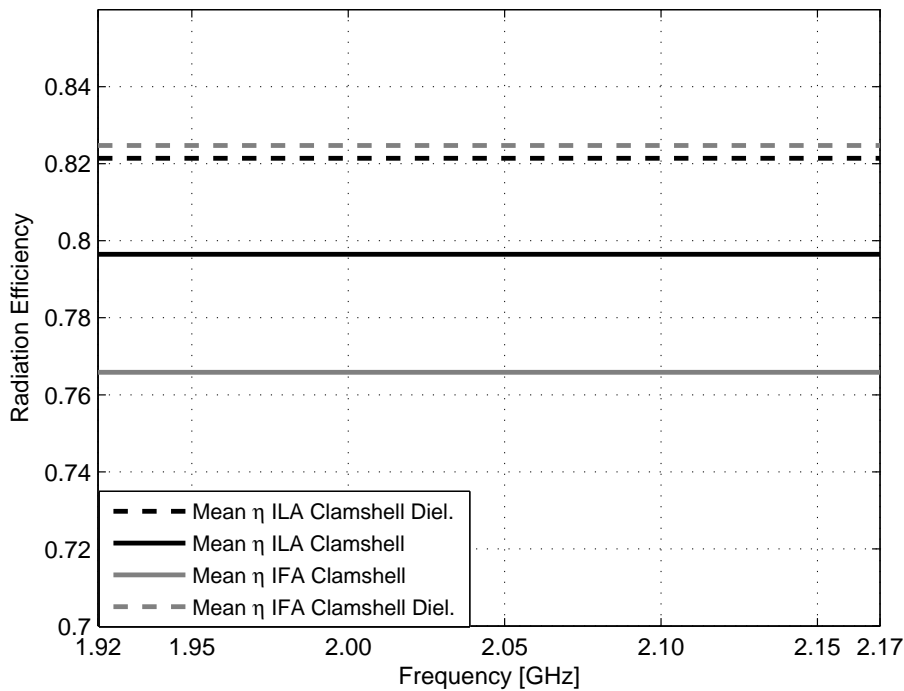


Figure 5.13: Total efficiency in a clamshell system with two antennas and two dielectric walls compare to systems with the same antennas, but without dielectric walls.

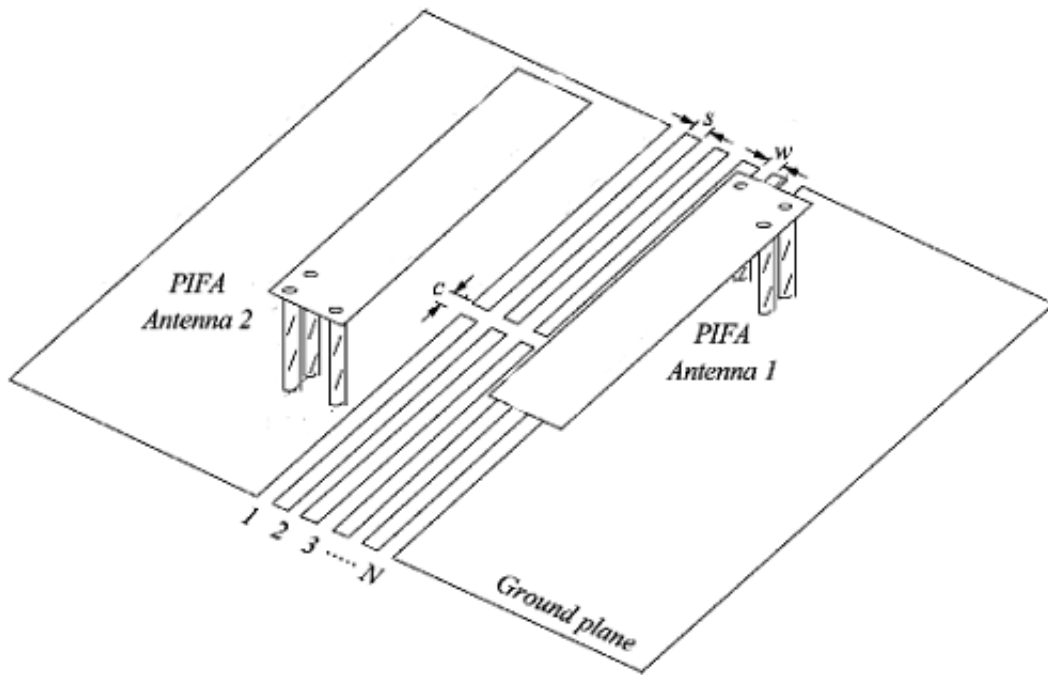


Figure 5.14: Geometry of two closely-packed PIFAs with slitted ground plane structure [7].

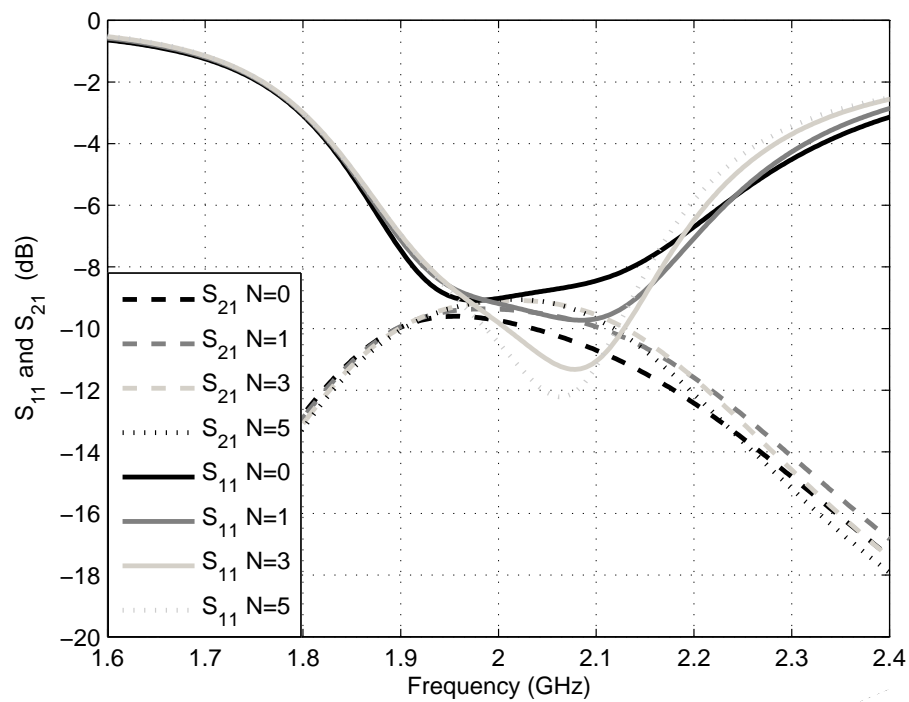


Figure 5.15: S_{11} and S_{21} in a two PIFA antenna system depending on the number of slits on either side of the ground plane.

The next parameter to modify is the distance between slits from different sides of the ground plane, with values of $c = 0, 4, 8, 30\text{mm}$ while $w = 1\text{mm}$, $s = 1\text{mm}$ and $N = 2$. As can be seen in Figure 5.16, the isolation barely improves. The value of the S_{11} parameter is lower when the slits are larger, i.e. when there is a small distance between the slits.

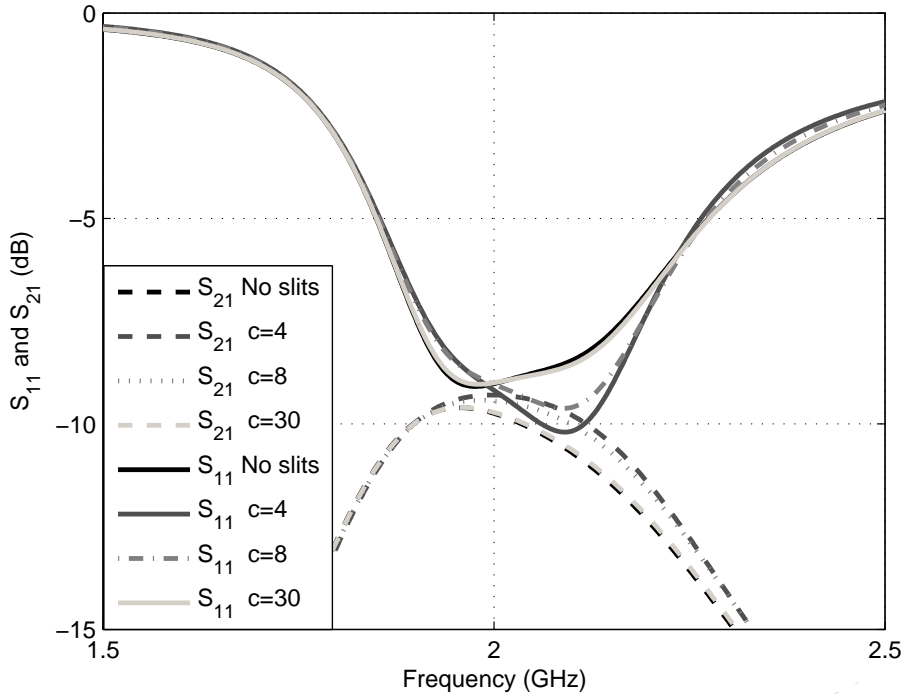


Figure 5.16: S_{11} and S_{21} in a two PIFA antenna system depending on the separation between the slits on either side of the ground plane.

The results obtained for the simulations with different values of the width of the slits, and the distance between the slits from the same side of the ground plane are given in Figure 5.17 and Figure 5.18 respectively. In the first case, a very good input impedance matching is reached when the slits are wider, getting an improvement of 5dB, but the isolating barely changes. However, changes in s has no influence in both matching and isolation.

Taking into account all the results given by the changes in the features of the slits, the proposed DGP with the same number of slits and the same position in both sides of the ground plane does not lead to an improvement in the isolation. The total efficiency in the best case of this DGP is 0.7954 while the total efficiency in a system with a normal ground plane is 0.7663. This value of the total efficiency is the mean value of the total efficiency calculated for all the frequencies within the bandwidth.

In the pursuit of improving the isolation, another DGP is tested. The difference with the prior DGP is that the slits are placed alternately, instead of being in the same position in both sides of the ground plane. The slits dimensions are $c = 2$, $s = 2$ and $w = 5$. This choice is based on the previous study, e.g. the slit is wider because the value of S_{11} is lower with the increases of the width. Figure 5.20 shows the geometry of this kind of DGP compared to other proposed DGPs and Figure 5.19 provides the input impedance matching and the isolation of these systems.

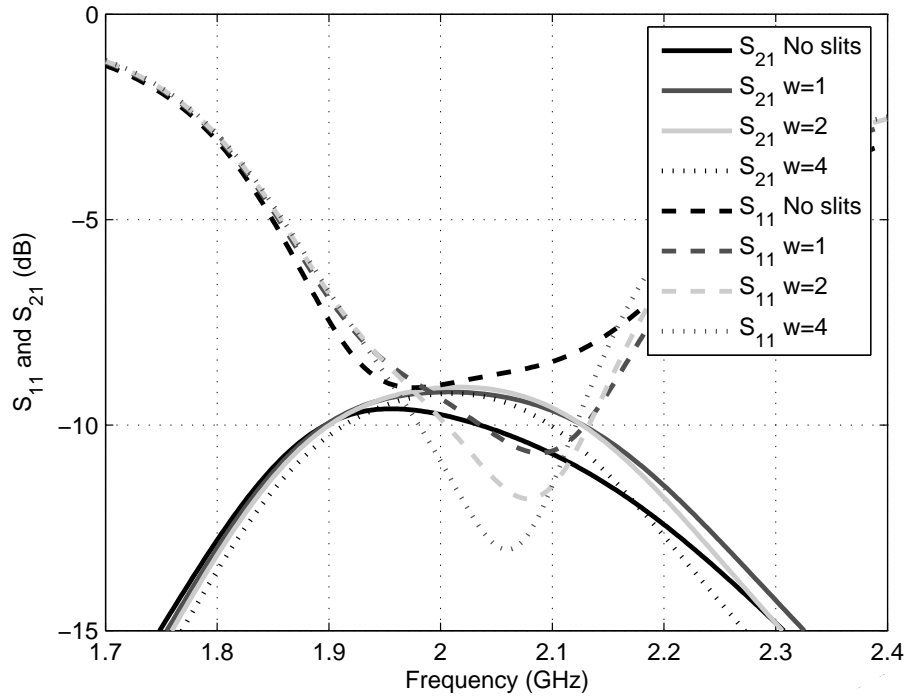


Figure 5.17: S_{11} and S_{21} in a two PIFA antenna system depending on the width of the slits.

From the results, this defected ground plane neither generates an improvement in the mutual coupling between the antennas. The total efficiency, in the best situation can reach the value of 0.7901 from 0.7663 that is the value for the system without slits. The problem is that the surface current has a path between the slits to access easily to the other part of the ground plane. Thereupon, another DGP with longer slits attached alternately is designed and presented in Figure 5.20. In this case, the current is forced to follow a meander path along the surface of the ground plane between the slits. Simulations with two and three slits are deployed and their results are given in Figure 5.21.

Based on the results, it can be seen that this slitted ground plane structure has a very positive impact on isolation. The input impedance matching is approximately the same for all the structures, but this geometry provides a significant improvement of isolation of 7.4 dB over the cases without slits. The explanation is that a large portion of surface current is being trapped by the first slit next to the radiating patch and thus less current is propagating across the slitted pattern. The total efficiency, as it was expected, has an increase too, reaching $\eta_T = 0.8287$ from the original value $\eta_T = 0.7663$. In Figure 5.22 are shown the total efficiencies of the antennas along the bandwidth and their mean value.

Finally, some structures with an irregular slitted pattern are designed. Once again, to reduce mutual coupling between the two antennas, the slits should hinder the passage of current from one side to the other side of the ground plane. Three structures are presented in Figure 5.23. The matching and the isolation of these three different DGPs are given in Figure 5.24. As seen in the graph, except for the first structure, the current flows from one side of the ground plane to the other side are substantially reduced and this effectively helps to reduce mutual coupling between

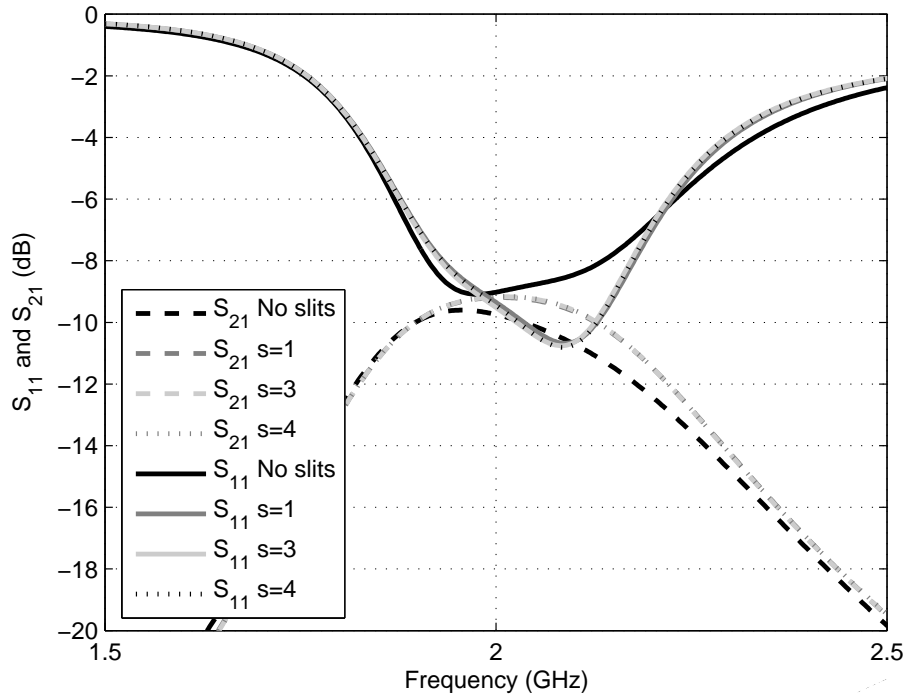


Figure 5.18: S_{11} and S_{21} in a two PIFA antenna system depending on the distance between the slits from the same side of the ground plane.

the two antennas. An improvement for the isolation of 6 dB and a total efficiency $\eta_T = 0.8262$ are achieved in the second case. In the third one, 7 dB and $\eta_T = 0.8264$.

According to the study of the defected ground planes, the conclusion is that those DGPs with a slitted pattern which obstructs the passage of current from one side to the other side of the ground plane, are good strategies to reduce the mutual coupling between antennas. To verify that it is not an exceptional case, the same DGP is tested in a system where transmission and reception are separated and in a system oriented for Clamshell mobile phones.

The designed DGP consists of two slits in the middle of the printed circuit board. Their width is 2mm , their length is 30mm and they are located alternately. The results in the separated transmission and reception system are depicted in Figure 5.25. Anew it is found that by applying the proposed slitted ground plane structure, the isolation between the antennas can be improved 7 dB as well. The envelope correlation for closely spaced antennas has to be low enough to make the diversity technique possible for implementation in the mobile handsets. The results of computing the correlation are provided in Figure 5.26, and they show the improvements in the system due to the DGP. It is achieved almost the half value of correlation of the initial system without slits.

The same procedure is followed for a ground plane that simulates the printed circuit board of a Clamshell mobile phone. As we already mentioned, the slits should be placed in the middle of the DGP. In addition to the antennas, other devices such as microphone, screen, battery, have to be located. Hence, in a normal ground plane with dimensions $100\text{mm} \times 40\text{mm}$, the space reserved for the slits is as much 10mm long. Nevertheless, in a clamshell, the dimensions of the

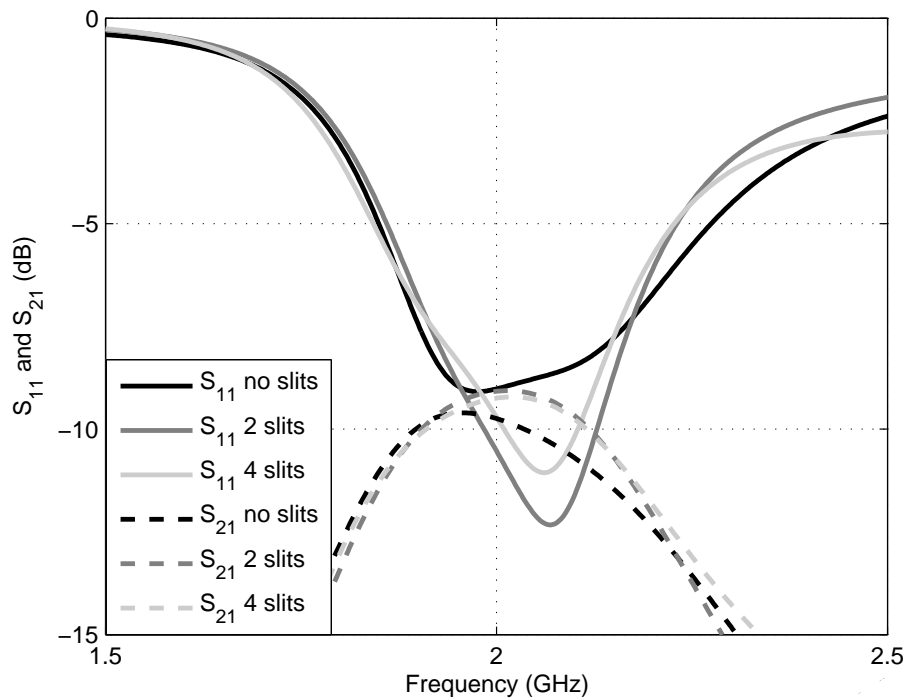


Figure 5.19: S_{11} and S_{21} in a two PIFA antenna system with slits placed alternately in the ground plane.

ground plane are $200\text{mm} \times 40\text{mm}$, so the space reserved for the slits can be around 20mm long. Consequently, the designed slits are wider (5mm). After seeing the results in Figure 5.27, the new system reaffirms this technique as a method to improve the isolation between antennas.

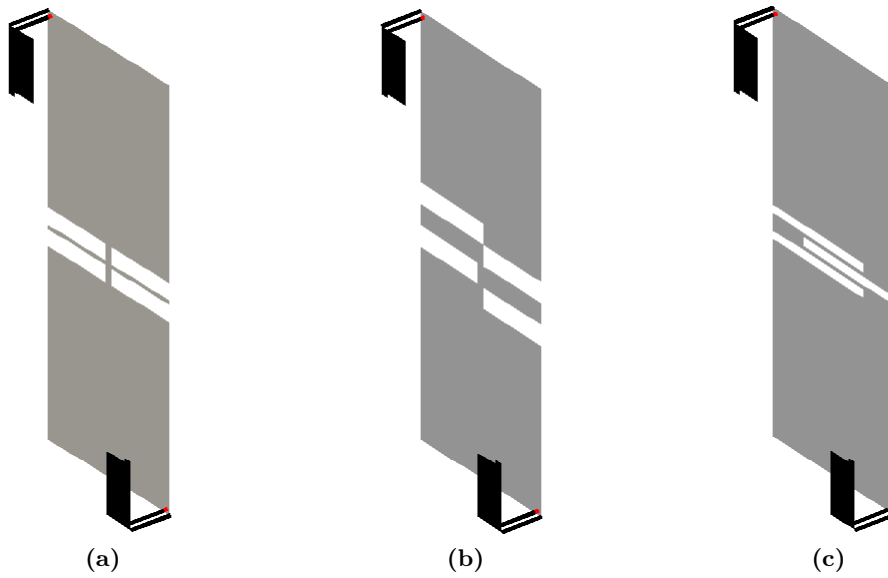


Figure 5.20: Different geometries of DGP. (a) slits in the same position in both sides. (b) slits placed alternately. (c) slits with a meander configuration

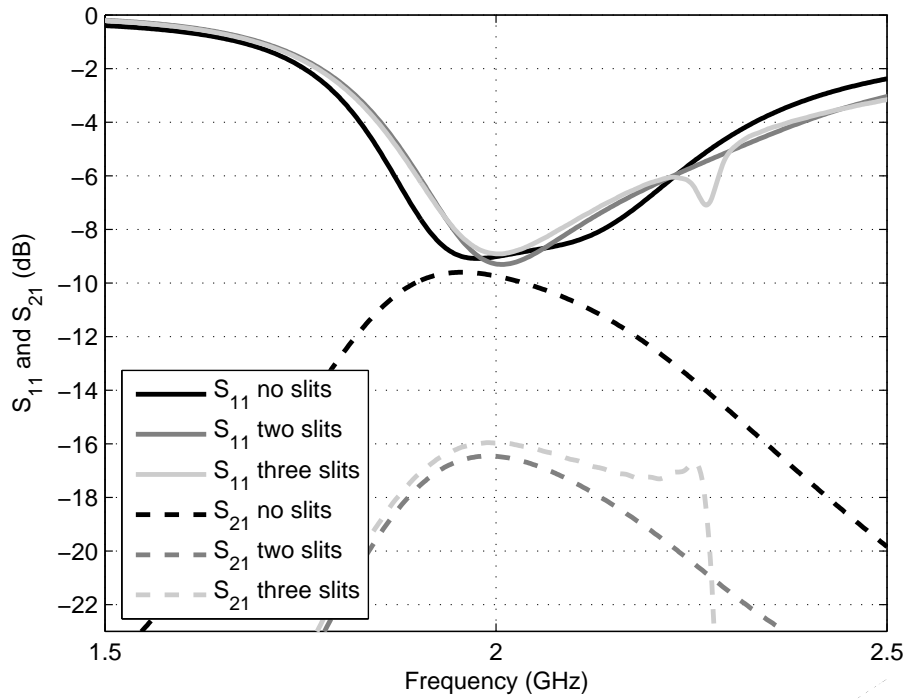


Figure 5.21: S_{11} and S_{21} in a two PIFA antenna system depending on the number of slits that are placed conceiving a meander path.

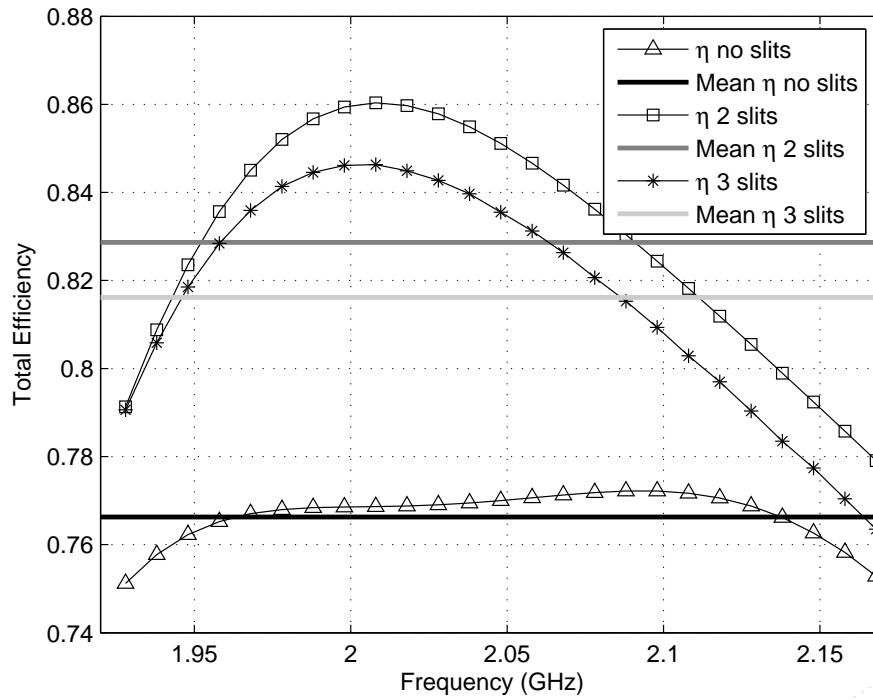


Figure 5.22: Total efficiency and its mean value in a two PIFA antenna system with a DGP with a meander slitted pattern.

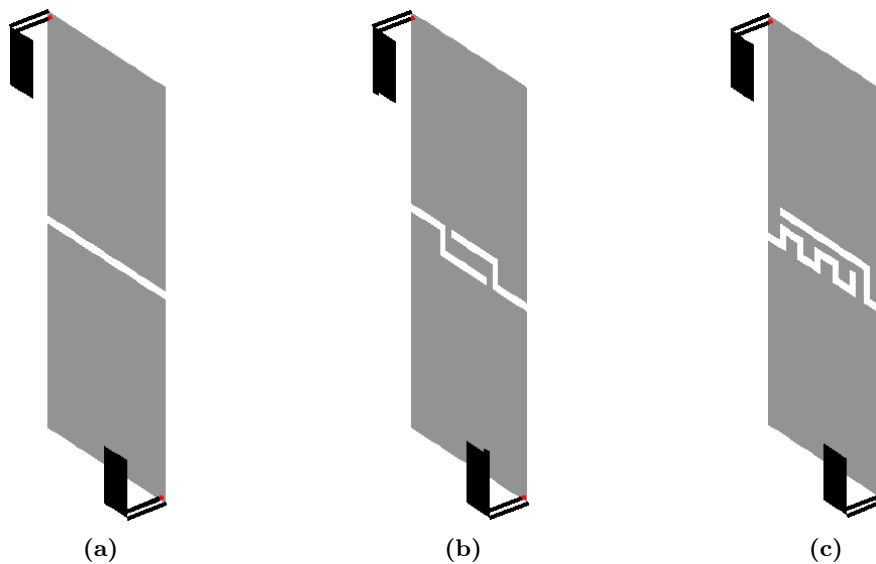


Figure 5.23: Different geometries of the DGP.

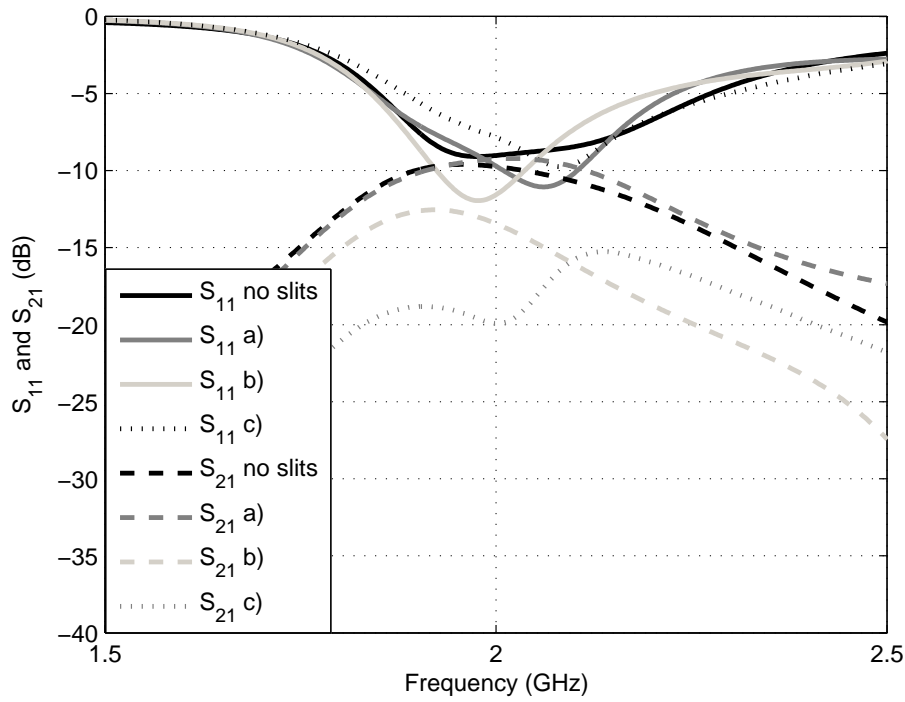


Figure 5.24: S_{11} and S_{21} in a two PIFA antenna system with a DGP with an irregular slitted pattern.

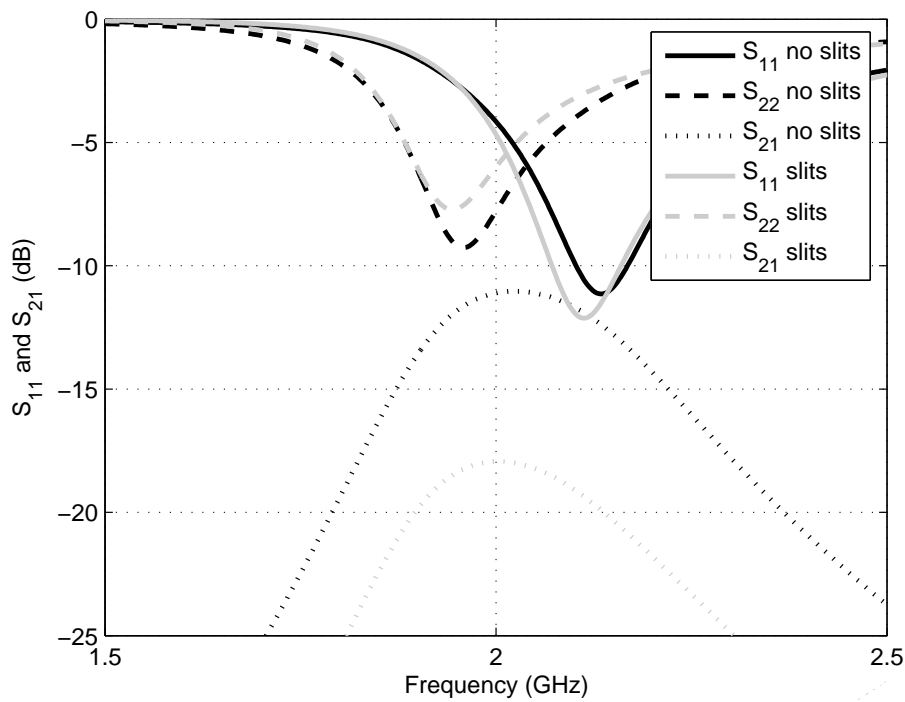


Figure 5.25: S_{11} and S_{21} in a system where transmission and reception are separated. The DGP is composed of two alternately slits in the middle of the ground plane.

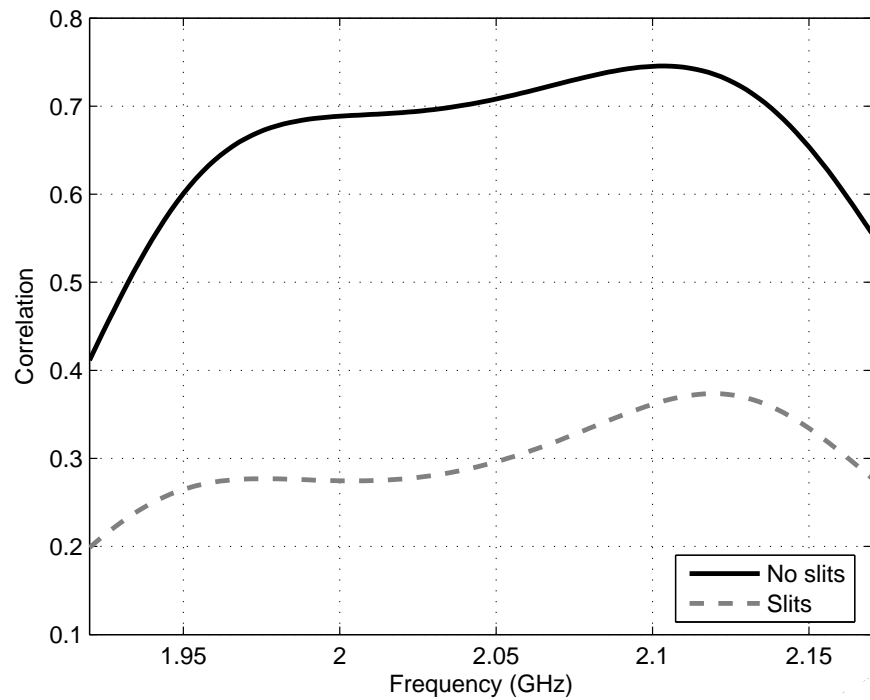


Figure 5.26: Correlation in a system where transmission and reception are separated. The system is tested with and without DGP.

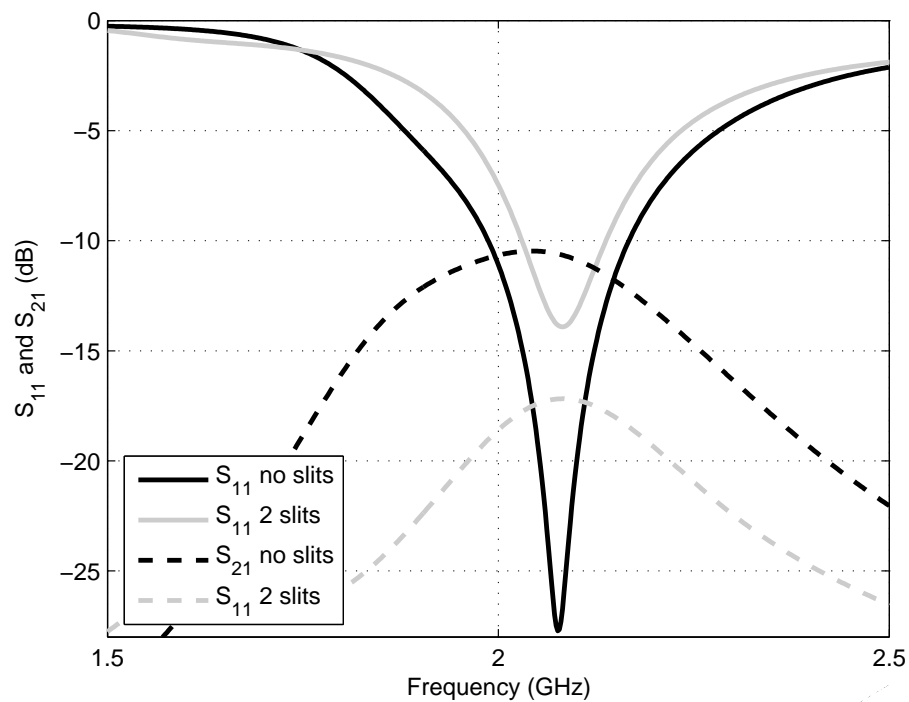


Figure 5.27: S_{11} and S_{21} in a clamshell with a DGP composed of two alternately slits in the middle of the ground plane.

Conclusions

The aim of this project was the investigation and determination of a novel way to reduce the mutual coupling and improve the isolation between two antennas in a diversity system for mobile communications.

A deeply study of the most common antennas for mobile handsets was done. Nowadays, Due to the dimensions of the mobile devices, small, compact and low profile antennas are required. For this reason inverted-L antenna (ILA), inverted-F antenna (IFA) and Planar inverted-F antenna (PIFA) are proposed. From this study, it is concluded that before choosing an antenna, it is necessary to achieve a good input impedance matching. Then, all the requirements related to the bandwidth and the resonance frequency can be obtained modifying the antenna parameters. Using that knowledge, antennas working on band I, band II and band V of UMTS technology were found.

Afterwards, two antennas were placed in the same printed circuit board to develop a diversity system. Three different types of systems were studied: one that used antennas which cover all the band I of UMTS, another where each antenna covered just half part of the bandwidth of UMTS band I, separating transmission from reception, and the third one that designed antennas for systems that simulates another kind of mobile phones, the so-called “clamshells”.

Finally, taking into account that when two antennas are located close each other, mutual coupling can occur between them. This can result in degradation of their radiation patterns and changes in the input impedance. Therefore, two methods to reduce mutual coupling and improve the isolation were introduced. The first one, consisted of two dielectric walls on the ground plane and between the antennas, did not lead to the desired results. The second one, provided a defected ground plane where the antennas were located. With this method, improvements up to 7 dB has been achieved.

For future works, it is proposed to repeat all the process and methods to improve the isolation for band II and band V of UMTS technology. Moreover, although the results were not the desired , they encourage us to think that the dielectric can become a good solution for mutual coupling problems.

Bibliography

- [1] <http://presse.aau.dk/nyheder/3353908>.
- [2] A. Diallo P. Le Thuc R. Staraj A. Chebihi, C. Luxey. A new method to increase the port-to-port isolation of a compact two-antenna umts system. (IEEE Antennas and Propagation Letters), March 2009.
- [3] D. Fernando Las-Heras Andres. Human exposure to electromagnetic emissions in mobile communications. June 2006.
- [4] C. A. Balanis. *Modern Antenna Handbook*. John Willey & sons, 2008.
- [5] bitsolution stalder. Speag, schmid and partner engineering ag. Website, 2005. <http://www.semcad.com/simulation/FDTD.php>.
- [6] C.C.-P. Chen, Tae-Woo Lee, N. Murugesan, and S.C. Hagness. Generalized fdtd-adi: an unconditionally stable full-wave maxwell's equations solver for vlsi interconnect modeling. pages 156–163, 2000.
- [7] Ross D. Murch Chi-Yuk Chiu, Chi-Ho Cheng and Corbett R. Rowell. Reduction of mutual coupling between closely-packed antenna elements. (IEEE transactions on antennas and propagation), June 2007.
- [8] Wolfgang J. R. Hoefer Daniel G. Swanson, Jr. *Microwave Circuit Modeling Using Electromagnetic Field Simulation*. ARTECH HOUSE, INC, 2003.
- [9] A. Constantinides A. Goldsmith A. PaulRaj H. Vincent Poor E. Biglieri, R. Calderbank. *MIMO Wireless Communications*. Cambridge University Press, 2007.
- [10] J.-D Xu F.-G. Zhu and Q. Xu. Reduction of mutual coupling between closely-packed antenna elements using defected ground structure. June 2009.
- [11] Y Fan Yang; Rahmat-Samii. Mutual coupling reduction of microstrip antennas usingelectromagnetic band-gap structure. (IEEE Antennas and Propagation Letters), 2001.
- [12] Ondrej Franek. *AAU3. Antennas, Propagation and Radio Networking*, Department of Electronic Systems. Aalborg University.

- [13] Min-Seok Han and Jaehoon Choi. Multiband mimo antenna with a band stop matching circuit for next generation mobile applications. August 2009.
- [14] Haridas. Pifa for mobile phones.
- [15] Aaron Kerkhoff. The calculation of mutual coupling between two antennas and its application to the reduction of mutual coupling effects in a pseudo-random phased array. August 2007.
- [16] H. Wong Mak, K.-M. and K.-M. Luk. A shorted bowtie patch antenna with a cross dipole for dual polarization. (IEEE Antennas and Wireless Propagation Letters), 2007.
- [17] Microwaves & RF. Achieving antenna isolation within wireless systems. <http://www.mwrf.com/>, 2003.
- [18] M. Pelosi, O. Franek, M.B. Knudsen, and G.F. Pedersen. Influence of dielectric loading on pifa antennas in close proximity to user's body. *Electronics Letters*, 45(5):246–247, 26 2009.
- [19] Edward M. Purcell. *Electrics and Magnetics*. Barkeley Physics Course. Volume 2, 1965.
- [20] K. Friedrichs R. Courant and H. Lewy. *On the partial difference equations of mathematical physics*. English translation of the 1928 German original, 1928.
- [21] J. Rahola and J. Ollikainen. Optimal antenna placement for mobile terminals using characteristic mode analysis. pages 1–6, Nov. 2006.
- [22] Inmaculada Tomeo Reyes. Application of high impedance surfaces to low profile wire antenna design. Master's thesis, Polytechnic School. Carlos III University. Madrid, June 2008.
- [23] C. A. s. *Modern Handbook*. John Willey & sons, 2008.
- [24] J. Romeu S. Blanch and I. Corbella. Exact representation of antenna system diversity performance from input parameter description. (Electronics Letters), May 2003.
- [25] Llewellyn I. Paul Smith, M. Stevens. Inverted-e antenna. (6025805), February 2000.
- [26] C. Soras, M. Karaboikis, G. Tsachtsiris, and V. Makios. Analysis and design of an inverted-f antenna printed on a pcmcia card for the 2.4 ghz ism band. *Antennas and Propagation Magazine, IEEE*, 44(1):37–44, Feb 2002.
- [27] Allen Taflove. *Electrodynamic The Finite Difference Time Domain Method*. ARTECH HOUSE, INC, 1995.
- [28] J. Villanen, J. Ollikainen, O. Kivekas, and P. Vainikainen. Compact antenna structures for mobile handsets. 1:40–44 Vol.1, Oct. 2003.
- [29] Ke Gong Yaxing Cai, Zhengwei Du. A novel wideband diversity antenna for mobile handsets. (Microwave and Optical Technology Letters), November 2008.
- [30] Lizhong Zheng and D.N.C. Tse. Diversity and multiplexing: a fundamental tradeoff in multiple-antenna channels. *Information Theory, IEEE Transactions on*, 49(5):1073–1096, May 2003.

Appendix

Evolution of mobile cellular network

To reach the current 3G mobile systems has been a long process. The first radiotelephone service was introduced in the United States at the end of the 1940s and in Europe in the early 1950s. This service connected mobile users in cars to the public fixed network, for example, in the police or taxi networks. It has many restrictions, as low capacity, limited service, and poor speech quality. Also the equipments were very heavy and expensive.

A.1 First-Generation Mobile Systems 1G

First Generation mobile phone networks were the earliest cellular systems to develop. These phones were still using analog radio channels (frequencies around 450 MHz), used for voice calls only, and their signals were transmitted by the method of frequency modulation (FM). This kind of phones had some disadvantages, such as a poor security due to the lack of encryption, and anyone with a receiver in the right frequency could hear the conversation.

The most prominent 1G systems are Advanced Mobile Phone System (AMPS), that was the first 1G system to start operating in the USA (in July 1978),, Nordic Mobile Telephone (NMT), and Total Access Communication System (TACS).

A.2 Second-Generation Mobile Systems 2G

Compared to first-generation systems, where radio signals were analog, in 2G networks radio signals are digital. They use digital multiple access technology, such as TDMA (time division multiple access) and CDMA (code division multiple access). 2G also introduced data services for mobile, starting with SMS text messages.

Examples of second-generation systems are GSM (Global System for Mobile Communications), Cordless Telephone (CT2), Personal Access Communications Systems (PACS), and Digital European Cordless Telephone (DECT)

A.3 Second and a half-Generation Mobile Systems 2.5G

The term "second and a half generation" is used to describe 2G-systems that have implemented a packet switched domain in addition to the circuit switched domain. This generation approaches 3G but with lower data rate. The generation 2.5G offers extended features, it has additional capacity on the 2G systems, such as GPRS (General Packet Radio System), HSCSD (High Speed Circuit Switched), EDGE (Enhanced Data Rates for Global Evolution). It offers wireless multimedia IP-based services and applications.

A.4 Third-Generation Mobile Systems 3G

The third generation (3G) is characterized by establishing the convergence of voice and data wireless Internet access, in other words, is suitable for multimedia applications and high data transmissions.

The protocols used in 3G systems support high speeds and are targeted for other applications apart from voice, such as audio (mp3), motion video, video conferencing and fast Internet access (string multimedia).

3G networks began operating in 2001 in Japan by NTT DoCoMo, and in Europe and parts of Asia in 2003. In Europe, there are three evolving networks under investigation: UMTS (Universal Mobile Telecommunications Systems), MBS (Mobile Broadband Systems), and WLAN (Wireless Local Area Networks).

A.5 Universal Mobile Telecommunications System UMTS

UMTS is one of the third-generation mobile telecommunications technologies. There are many radio spectrum frequencies designated for the operation of the UMTS. This project was supposed to work with the frequencies for band I, II and V, which are shown in the table.

Operating Band	Frequency Band	Common name	UL (MHz)	DL (MHz)	Region
I	2100	IMT	1920-1980	2110-2170	Europe, Asia, Korea, Japan, Australia, New Zealand, Brazil
II	1900	PCS	1850-1910	1930-1990	North America
V	850	CLR	824-849	869-894	North America, Australia, New Zealand, Philippines, Brazil

Table A.1: Frequency bands for UMTS.

Appendix B

Monopole Theory

Monopoles are vertical antennas over a ground plane with a source, connected also to the ground plane, at its bottom. As is explained by the reflections theory [4]. The reflections of the radiated

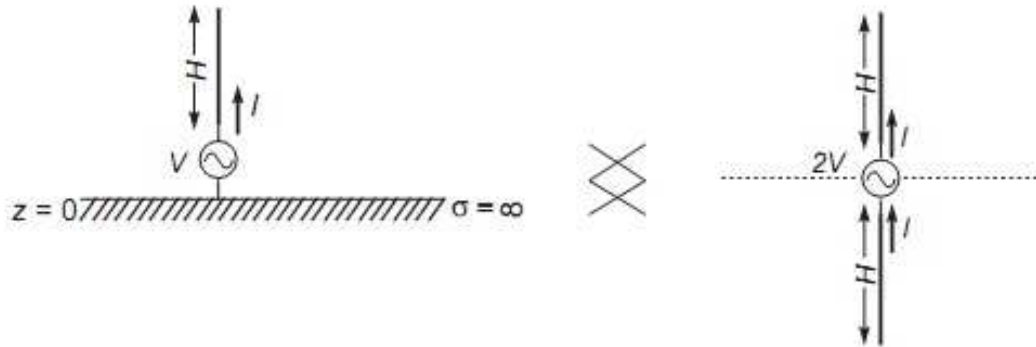


Figure B.1: monopole and dipole

energy by the monopole, on the ground plane, which we consider is a perfect conductor, can be considered as the radiated energy from the space under the ground plane (figure 2). This fact is the principle used to create a 'virtual monopole' under the ground plane [23]. Finally if we consider the monopole with a length, H, and its reflection over the ground plane we obtain a dipole which total length is 2H, as you can see at B.1. In the space over the ground monopole radiates fields equals than a dipole with the same length as monopole, so we will have the same intensity distribution and radiation pattern. In the table below we show some other monopole features comparing with dipoles:

- $P_{rmono} = \frac{1}{2}P_{rdipole}$
- $R_{rmono} = Pr/I(0) = 1/2R_{rdipole}$
- $V_{mono} = 1/2V_{dipole}$
- $D_{mono} = 2D_{dipole}$

- $A_{efmono} = 1/2A_{efdipole}$
- $l_{efmono} = 1/2l_{efdipole}$

As monopoles only radiates in the upper space it has the double directivity as dipole, but on the contrary has the half power radiated P_r and consequently half radiation impedance R_r .

The monopoles antennas are mainly used at low frequencies (30 KHz - 3000 KHz) where the wavelength is too long to build antennas as dipoles. Of course they are used also in UHF and microwave frequencies. Microwaves range is the one we are going to use for mobile applications. Typically the antenna is one half or a quarter of wavelength in length along at least one axis and this length for GSM applications is still too longer. The following kind of monopoles tries to reduce the height of monopole but keeping maintaining its resonant trace length.

B.1 Inverted-L Antenna ILA

One of this monopole is the Inverted-L Antenna. It is still a monopole that has been folded down, so one part of it is parallel to the ground. It could be considered as a vertical short monopole with an horizontal wire attached at the end of the monopole. The height of the vertical element is usually constrained to a fraction of the wavelength. The total length including vertical and horizontal arms is usually a quarter of wavelength [25]. The ILA has inherently low impedance, since the antenna is a short monopole loaded with a long horizontal wire at the end of the monopole. The input impedance is nearly equal to the sum of the short monopole impedance and the reactance of the horizontal wire that is closely placed to the ground plane. Figure B.2 represents a scheme of the antenna. Moreover, this antenna produces both vertical and horizontal polarized electrical fields which is desirable for indoor environments [4] .

B.2 Inverted-F Antenna IFA

A simple and typical modification of an ILA is an Inverted-F Antenna (IFA). A small ILA element is attached at the end of the vertical element of an ILA and the appearance is that of a letter F facing the ground plane. Figure B.2 shows the shape of an IFA antenna.

ILA antenna is difficult to match because its impedance consists of a small resistance and a high reactance. Due to the mismatch the radiation efficiency of the antenna decreases considerably. Therefore, it is necessary to add something to achieve a virtually resistive input impedance that fits easily into a standard coaxial line. For this reason, a shorting circuit is added and thus providing an IFA antenna. This modification can allow the input impedance to have an appropriate value just changing the distance between the new element and the source.

B.3 Planar Inverted-F Antenna PIFA

PIFA is a kind of linear Inverted-F antenna (IFA) with the wire radiator element replaced by a plate to expand the bandwidth [14]. Hence, as shown in Figure B.2, the PIFA consists of a ground plane, a top plate element, a feed wire attached between the ground plane and the top plate, and a shorting wire or strip that is connected between the ground plane and the top plate.

PIFA antenna has many advantages, that is, easy fabrication, low manufacturing cost, and simple structure. PIFA can be hiding in the housing of the mobile phone when comparable to whip, rod or helix antennas. Besides, PIFA has reduced backward radiation towards the user's head, minimizing the electromagnetic wave power absorption (SAR). But the major disadvantage that keeps the basic PIFA from diverse applications is its narrow bandwidth.



Figure B.2: Antenna Schemes.

Finite-Differences Time-Domain FDTD

Finite Differences in Time Domain method FDTD is one of the many methods used in computational electromagnetic. It is used for solving transient electromagnetic problems using finite differences. The method, based on a spatial and temporal discretization of Maxwell's curl equations, was developed by Kane Yee in 1966 [8]. These partial differential equations are replaced by a system of finite difference equations. Conveniently choosing the points at which assesses the field components in these equations, the solution satisfies the boundary conditions involving ideal conducting surfaces.

Maxwell's equations describe the evolution in time and space of the magnetic and electric fields. As it is described in [27], following Yee's algorithm, the time-dependent Maxwell's equations are discretized using central-difference approximations to the space and time partial derivatives. Consequently, with this equations, future values of the H -field components can be computed from their previous values and the present spatial variations of the E -field, and vice versa. It is necessary to define appropriate initial and boundary conditions before the update process begins.

The sampled values of the electric and magnetic field have to be staggered in space and time to obtain central difference approximations of Maxwell's equations. To get these discrete samples in space, it is necessary to define a numerical grid stored in the computer memory. Commonly it is a rectilinear cartesian grid, where the basic element is the Yee's cell which is shown in Figure C.1 . As they have to be staggered, the positions of the electric field samples are defined half way between those of the magnetic field samples. Therefore, the corner of a cube belonging to the E -field grid is located in the centre of a cube belonging to the H -field grid, thus each E component is surrounded by four H components and vice versa, which leads to a spatially coupled system of field circulations corresponding to the law of Faraday and Ampere. Each three E - and H -field components are assigned to a node i, j, k within the three dimensional FDTD grid. The same happens in time, if the electric field components are sampled at the discrete time point t then the magnetic field components are sampled at time points $t + 1/2$, as it can see in Figure C.2.

As it already mentioned, it is necessary to define appropriate boundary conditions for a conducting surface, i.e. the tangential components of the electric field and the perpendicular component of the magnetic field vanish on the surface. As there is not any information from outside the existing FDTD grid, it is not possible to determine, using differential equations, the tangential field components located at the domain boundaries. To solve that, Absorbing Boundary Conditions ABC are used. These methods are based on two principles: conditions imitating an absorbing material or conditions based on plane wave solutions to the wave equation.

The size of the grid should be such that electromagnetic fields do not change substantially from one node to another in the grid. This means that to have significant results, the grid dimension must be a fraction of the wavelength λ . Typically, 10 to 20 samples per cycle [6].

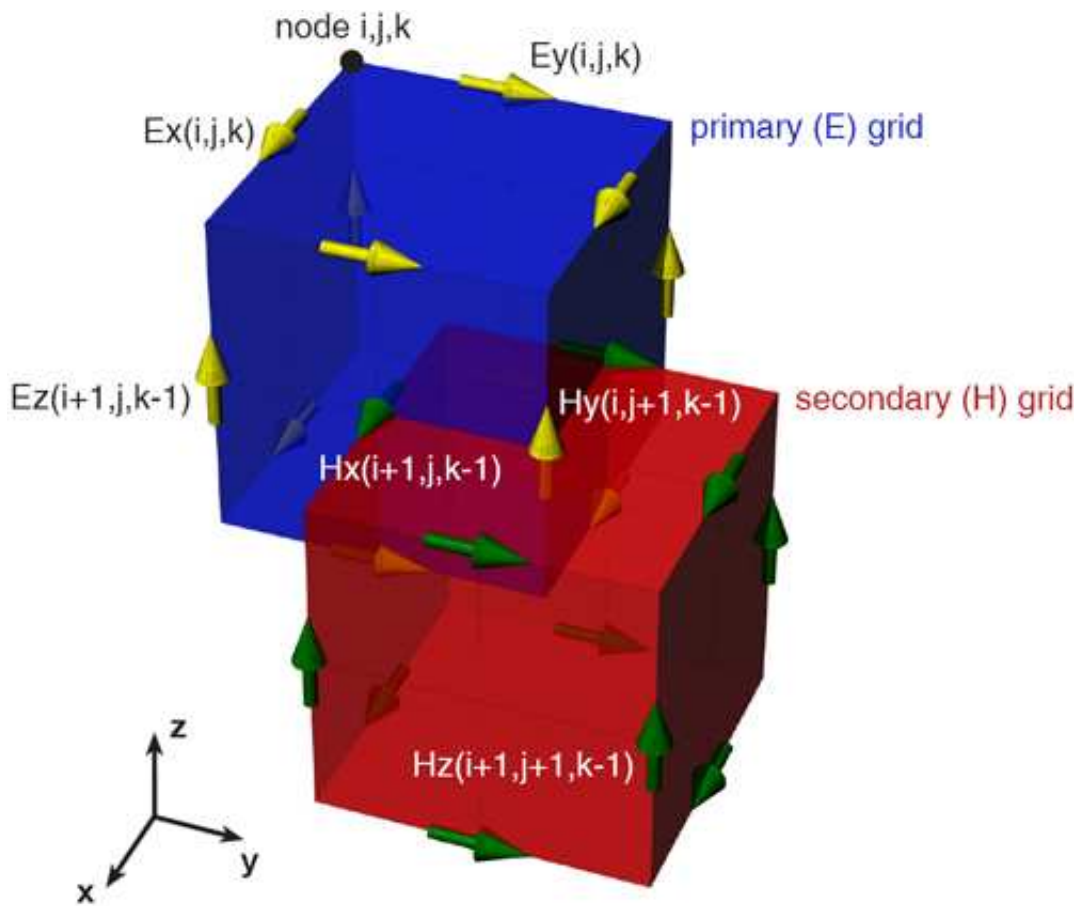


Figure C.1: 3D primary and secondary cell within Yee grid in FDTD representing E - and H -field components in the discretized space [5].

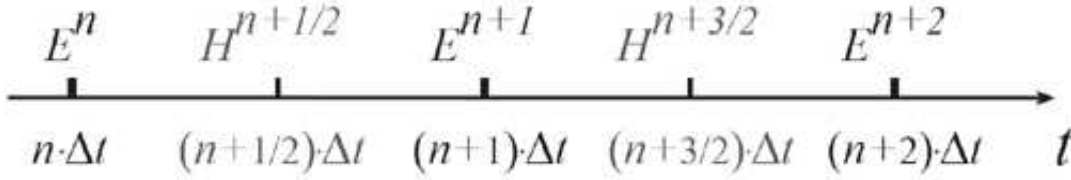


Figure C.2: Leap-frog scheme in FDTD: temporal updating of electric and magnetic field components using half a time step temporal separation [5].

The numerical stability of the solution requires a bounding of the time step relative to the space increment, given by the criterion of Courant [20] which, for 3D, establishes the following condition:

$$\Delta t = \frac{1}{c \cdot \sqrt{\frac{1}{(\Delta x)^2} + \frac{1}{(\Delta y)^2} + \frac{1}{(\Delta z)^2}}} \quad (\text{C.1})$$

where c is the speed of wave propagation in free space. For a computational domain consisting of cubic grid cells of space increment Δ , this stability limit simplifies to $\Delta t \leq \Delta / (c\sqrt{3})$

C.1 3rd generation FDTD program

All the simulations that were made throughout this project have used the AAU3 software that was written in Matlab high-level. This program allows to design antennas and then generates the main output parameters in electromagnetics (radiation patterns, impedance, smith chart, radiation efficiency, etc.). The code is based on the FDTD and there are two possibilities of running the simulations: either by Matlab kernel or by Fortran FDTD kernel, which is faster compared in the compilation duration.

The user interface consists of two windows: the main window, where the input parameters of the antenna system can be defined, and the geometry window, where the geometry of the system is displayed. In Figure C.3 both windows are shown, with a typical structure used in this project. Further information related on how to use the software is written in the manual of the AAU3 [12].

It is possible to add perfectly matched layers (PML) beyond the actual boundaries, so that the waves radiated from the antenna are not bounced back and the antenna is virtually placed in free space.

The most important part of the AAU3 program is the results menu, where all the parameters that describe the antenna system can be checked. Figure C.4 shows this menu. To compute all the results AAU3 implements the excitation source as a resistive source connected to the Yee grid in place of one component of the electric field. Situation with z -oriented source is depicted in Figure C.5, where V_s is the excitation pulse applied as the source voltage, V is the input voltage, R_s is the source impedance fixed to 50 and I is the input current, i.e. the current flowing from the source to the simulation domain.

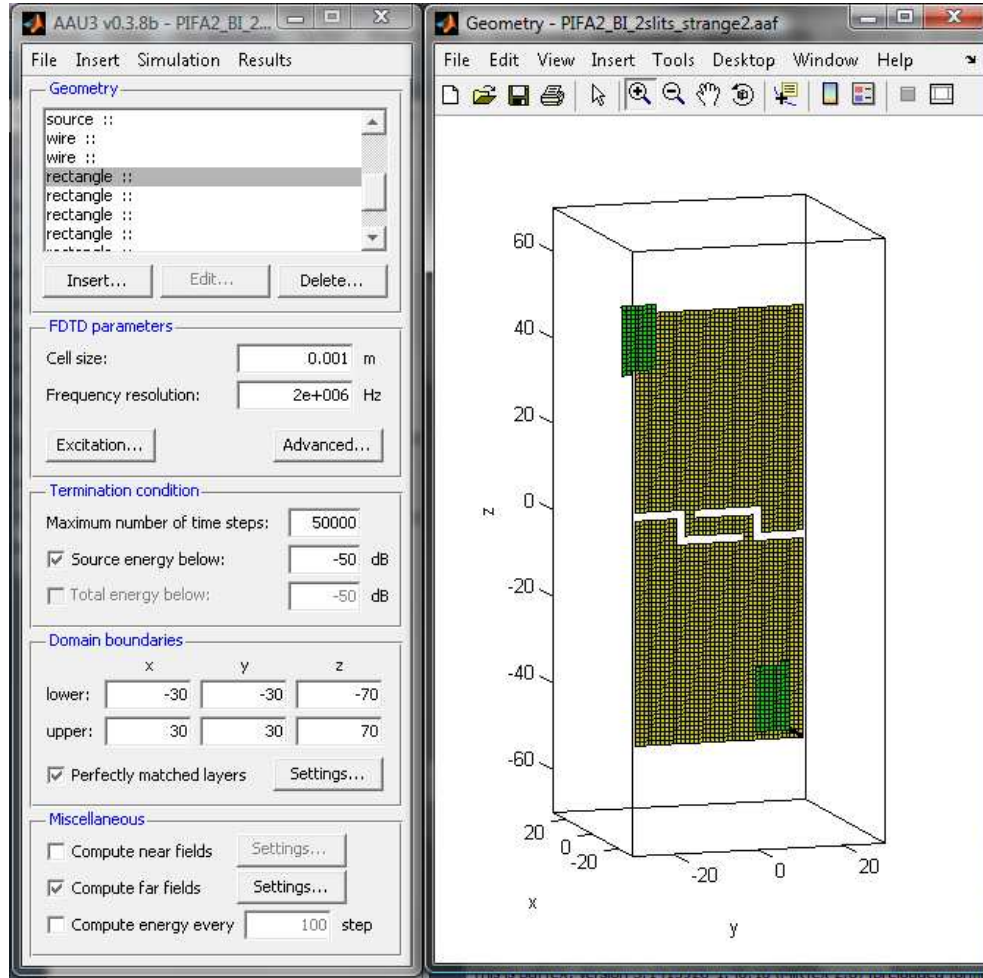


Figure C.3: AAU3: The main window (left) and Geometry window (right).

The input voltage is obtained in the FDTD code as a voltage across the source area, i.e. along the edge of the Yee cube. Once V is calculated, the input current can be obtained using the equation

$$I = \frac{V + V_s}{R_s} \quad (\text{C.2})$$

the impedance Z is obtained as

$$Z = -\frac{V}{I} = -\frac{R_s}{1 + V_s/V} \quad (\text{C.3})$$

and the S_{11} parameter as

$$S_{11} = \frac{Z - R_s}{Z + R_s} \quad (\text{C.4})$$

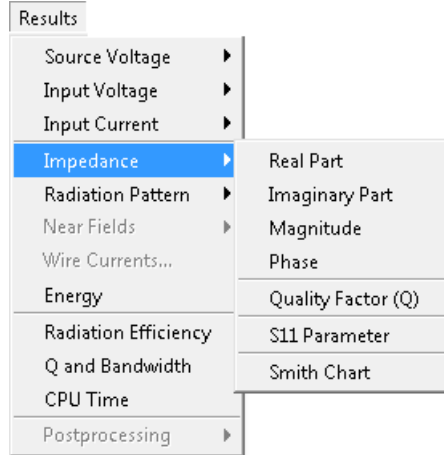


Figure C.4: Results menu.

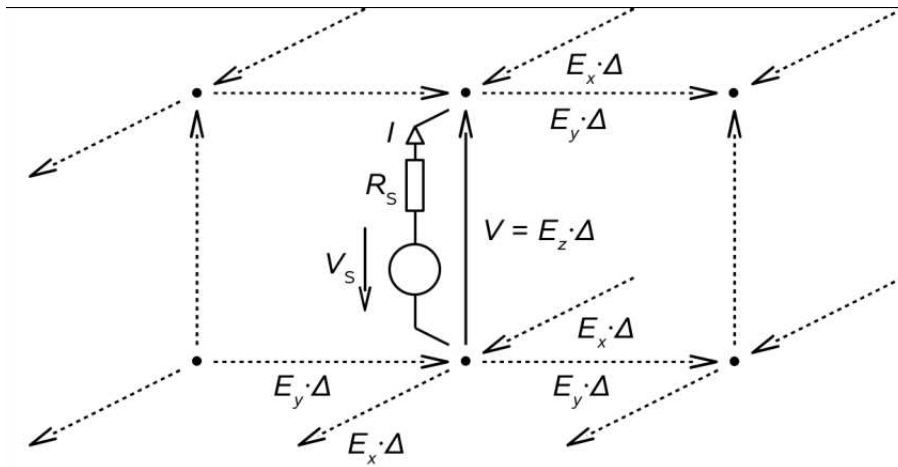


Figure C.5: Resistive source incorporated in the Yee grid [12].

Starting from the differential form of the Ampere's law, assuming an homogeneous cubical Yee grid ($\Delta = \Delta x = \Delta y = \Delta z$) and discretizing by central differences in a time instant $t = n + 0.5$ for a source oriented in z direction [12], it is obtained the resulting update equation for the vertical electric field E_z

$$E_z^{(n+1)} = \frac{1 - \frac{\Delta t}{2\epsilon R_s \Delta}}{1 + \frac{\Delta t}{2\epsilon R_s \Delta}} E_z^{(n)} + \frac{\frac{\Delta t}{\epsilon}}{1 + \frac{\Delta t}{2\epsilon R_s \Delta}} \nabla \times \vec{H}^{(n+0.5)} - \frac{\frac{\Delta t}{\epsilon R_s \Delta^2}}{1 + \frac{\Delta t}{2\epsilon R_s \Delta}} V_s^{(n+0.5)} \quad (C.5)$$

where R_s represents the integral value of conductivity over the whole Yee cell.

$$R_s = \frac{1}{\sigma \Delta} \quad (C.6)$$

In the frequency domain, to compute the results it is used the discrete Fourier transform (DFT). The input voltage (or the input current) is saved as a sequence of samples in time which are

transformed in frequency domain by FFT algorithm with the following relation:

$$\Delta t \cdot \Delta f \cdot N_t = 1 \tag{C.7}$$

where

- Δt : Time step, given by the Courant-Friedrichs-Lewy condition or specified manually
- Δf : Frequency resolution.
- N_t : Number of samples.

MIMO Systems

MIMO (Multiple-Input Multiple-Output) means that several transmitters and receivers can be used at each end of the radio link in order to achieve a high capacity. In other words, a transmitter with two antennas can send data simultaneously by two different paths so the speed can be double. The 802.11n uses MIMO to reach theoretical speeds upper than 600 Mbits, i.e. the bit rate is double than actual wireless standards as 802.11a and 802.11g.

Depending on the number of antennas at the transmitter and receiver. Variations of MIMO can be distinguished from the list below and in Figure D.1 :

- MIMO: Several antennas are placed at the transmitter and receiver.
- MISO: Several antennas are placed in the transmitter but only one in the receiver.
- SIMO: Only one antenna is placed in the transmitter and several are located in the receiver.
- SISO: Only one antenna is placed in both the transmitter and the receiver.

D.1 Fundamentals of MIMO

multi-path scattering commonly has been seen as an impediment to classical wireless communications. The fundamental of MIMO systems is to take advantage of this. Multipath means that the signals can arrive to the receiver from different paths in different times. Also the frequency and even the level of energy can be different due to the scattering of the electromagnetic waves in the environment [9].

Traditionally, multiple antennas have been used to increase diversity and thus combat channel fading. Each pair of transmitting and receiving antennas provides a path for the signal from the transmitter to the receiver. By sending signals with the same frequency and the same information through different paths, multiple independent replicas of the data can be obtained at the receiver; hence, more reliable reception is achieved [30]. This is the performance of MIMO. MIMO systems base its extraordinary capacity and spectral efficiency in environments where

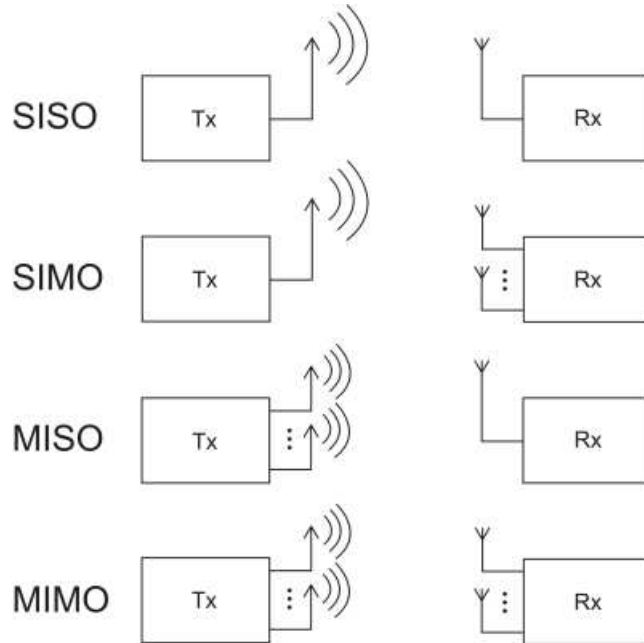


Figure D.1: Scheme of the variants of MIMO

signal paths are uncorrelated and this is especially common in dispersive environments.

The main requirement for MIMO systems is that the antennas must be able to receive different signals, even though if they are closely spaced. The different signal paths should be uncorrelated to ensure a good diversity gain and the mutual coupling has to be as less as possible to avoid the energy transfer between antennas and therefore, the increase of the correlation.

Due to this requirements, implement MIMO systems in mobile phone is nowadays still a challenge, because it is difficult to add multiple antennas on something so small and pretend to have a good isolation. Another feature is that the performance of the antenna will be degraded by the effects of inter-antenna coupling, envelope cross-correlation and coupling to biological tissues in the user's hands.

D.2 Benefits of MIMO technology

In this section benefits of MIMO technology are described [9].

Array gain

Array gain is the increase in receive SNR (Signal Noise Rate) that results from a coherent combining effect of the wireless signals at a receiver. The coherent combining may be realized through spatial processing at the receive antenna array and/or spatial pre-processing at the transmit antenna array. Array gain improves resistance to noise, thereby improving the coverage and the range of a wireless network.

Spatial diversity gain

As mentioned before, the signal level at a receiver in a wireless system fluctuates or fades. The spatial diversity gain mitigates fading and it is realized by providing the receiver with multiple (ideally independent) copies of the transmitted signal in space, frequency or time. With an increasing number of independent copies (the number of copies is often referred to as the diversity order), the probability that at least one of the copies is not experiencing a deep fade increases, thereby improving the quality and reliability of reception. A MIMO channel with M_T transmit antennas and M_R receive antennas potentially offers $M_T M_R$ independently fading links, and hence a spatial diversity order of $M_T M_R$.

Spatial multiplexing gain

MIMO systems offer a linear increase in data rate through spatial multiplexing, i.e., transmitting multiple, independent data streams within the bandwidth of operation. Under suitable channel conditions, such as rich scattering in the environment, the receiver can separate the data streams. Furthermore, each data stream experiences at least the same channel quality that would be experienced by a single-input single-output system, effectively enhancing the capacity by a multiplicative factor equal to the number of streams. In general, the number of data streams that can be reliably supported by a MIMO channel equals the minimum of the number of transmit antennas and the number of receive antennas, i.e., $\min(M_T, M_R)$. The spatial multiplexing gain increases the capacity of a wireless network.

Interference reduction and avoidance

Interference in wireless networks results from multiple users sharing time and frequency resources. Interference may be mitigated in MIMO systems by exploiting the spatial dimension to increase the separation between users. For instance, in the presence of interference, array gain increases the tolerance to noise as well as the interference power, hence improving the signal-to-noise-plus-interference ratio (SINR). Additionally, the spatial dimension may be leveraged for the purposes of interference avoidance, i.e., directing signal energy towards the intended user and minimizing interference to other users. Interference reduction and avoidance improve the coverage and range of a wireless network.

In general, it may not be possible to exploit simultaneously all the benefits described above due to conflicting demands on the spatial degrees of freedom. However, using some combination of the benefits across a wireless network will result in improved capacity, coverage and reliability.